Eur. Phys. J. C (2010) 69: 241–263
DOI 10.1140/epjc/s10052-010-1401-8

THE EUROPEAN PHYSICAL JOURNAL C

Regular Article - Theoretical Physics

Tachyonic γ-ray bursts generated by nonlocal plasma currents

Roman Tomaschitz[a]

Department of Physics, Hiroshima University, 1-3-1 Kagami-yama, Higashi-Hiroshima 739-8526, Japan

Received: 8 March 2010 / Published online: 13 August 2010

Abstract The dispersion relations of superluminal wave propagation in electron plasmas are derived, and the tachyonic energy flux, the velocity of energy transport, and the relaxation time asymptotics of the conductivity are studied. The formalism is based on Maxwell-type equations for Proca fields with negative mass-square in dispersive and dissipative media. Specifically, superluminal radiation fields generated by the ultra-relativistic electronic source plasma of γ-ray bursts (GRBs) are investigated. The radiation field is coupled to the shock-heated electron gas by a frequency-dependent fine-structure constant. The varying coupling constant generates long-range dispersion in the charge and current densities. At high energy, the coupling strength approaches a finite limit, so that the Proca field becomes minimally coupled to the electron current. The tachyonic fine-structure constant scales with the frequency-dependent superluminal velocity of the radiated modes. This scaling is manifested in the tachyonic flux densities of the GRB plasma, so that the scaling exponent can be extracted from spectral maps in the soft γ-ray band. To this end, tachyonic spectral fits of GRB 930506, GRB 950425, and GRB 910503 are performed. The scaling amplitude of the fine-structure constant is inferred from the burst duration. The transversal and longitudinal tachyonic luminosity of the source plasma is calculated in the high-temperature regime. Estimates of the plasma temperature and the internal energy of the ultra-relativistic electron gas are obtained.

1 Introduction

We investigate superluminal wave propagation in γ-ray burst (GRB) plasmas, where the tachyonic Maxwell–Proca equations have to be supplemented by material equations. The formalism is developed in analogy to the electromagnetic theory of dispersive and dissipative media, based on permeabilities and inductions. In contrast to vacuum fields, the dispersion relations for transversal and longitudinal wave propagation differ in a permeable medium, and the tachyonic wavelength can exceed the Compton wavelength $2\pi/m_{\mathrm{t}}$, where $m_{\mathrm{t}} > 0$ is the tachyon mass. This is not possible in vacuum, due to the mass-square in the dispersion relation $2\pi/\lambda = \sqrt{\omega^2 + m_{\mathrm{t}}^2}$. We analyze the effect of dispersion and absorption on the tachyonic energy and flux densities, calculate the group velocity and attenuation length of the superluminal modes, and show that the tachyonic transparency of an electron plasma depends on the polarization of the radiation.

We study tachyonic Proca fields [1–3] coupled to electron currents by a frequency-dependent coupling constant resulting in a nonlocal interaction. The varying coupling constant generates long-range dispersion of the charge and current densities in the vacuum field equations, so that the singular densities of a point charge become extended. The coupling constant scales with the velocity of the tachyonic modes, $q = q_{\mathrm{t}}\upsilon_{\mathrm{t}}^{\sigma}(\omega)$. The scaling exponent σ can be extracted from the low-energy slopes of GRB spectra, and the scaling amplitude q_{t} is estimated from the burst duration by balancing the tachyonic luminosity with the internal energy of the electronic source plasma. In the high-frequency limit, the radiation modes become minimally coupled to the current. The group velocity $\upsilon_{\mathrm{t}} = \sqrt{1 + m_{\mathrm{t}}^2/\omega^2}$ of the superluminal vacuum modes depends on their frequency and the tachyon mass m_{t}, and converges to the speed of light at high frequency, so that the minimal coupling in the high-energy regime $\omega/m_{\mathrm{t}} \gg 1$ is determined by the scaling amplitude q_{t} [3].

Tachyonic radiation implies superluminal signal transfer [4–9], the energy quanta propagating faster than light in vacuum, in contrast to rotating superluminal light sources emitting vacuum Cherenkov radiation [10–13]. This superluminal energy propagation by tachyonic modes is also to be distinguished from superluminal group velocities arising in photonic crystals, optical fibers, or metamaterials [14–16]. In contrast to tachyonic quanta, the actual signal speed defined by the electromagnetic energy flow in these media is

[a] e-mail: tom@geminga.org

always subluminal and occasionally even opposite to the group velocity [17, 18].

In Sect. 2, we set up the formalism of tachyonic Proca and Maxwell fields in a permeable space. In Sect. 3, we derive the dispersion relations for transversal and longitudinal wave propagation, and investigate superluminal energy transport with frequency-dependent permeabilities. Dissipation is accounted for by complex permeabilities resulting in exponential attenuation of the tachyonic radiation modes. In Sect. 4, we explain the nonlocal interaction of tachyonic radiation fields with electron currents. We develop the formalism in Fourier space and real time, and analyze the dispersion caused by the energy-dependent coupling constant.

The transversal and longitudinal tachyonic conductivity of an electron plasma is studied in Sect. 5, by making use of the relaxation time asymptotics of the dispersion relations. In Sect. 6, we discuss the superluminal radiation densities of ultra-relativistic electrons, the spectral averaging over electronic power-law distributions, and the effect of the frequency-dependent fine-structure constant on the spectral functions. We assemble the transversal and longitudinal tachyonic flux densities, and perform spectral fits to the γ-ray bursts GRB 930506, GRB 950425, and GRB 910503 [19]. In Sect. 7, we discuss the superluminal power transversally and longitudinally radiated by ultra-relativistic electrons, in particular the tachyonic luminosity of GRB plasmas. In Sect. 8, we present our conclusions. In Appendix A, we calculate the time asymptotics of the nonlocal charge density in the Proca equation. In Appendix B, we derive the high-temperature expansion of the tachyonic luminosity of thermal and nonthermal electron plasmas.

2 Proca fields with negative mass-square: tachyonic field strengths, inductions, and constitutive equations

The tachyonic radiation field is a real Proca field $(\hat{A}_0, \hat{\mathbf{A}})$ with negative mass-square [20, 21], coupled to the electron current by minimal substitution. We will mostly consider monochromatic fields, $A_0(\mathbf{x},t) = \hat{A}_0(\mathbf{x},\omega)\mathrm{e}^{-\mathrm{i}\omega t} + \text{c.c.}$, $\mathbf{A}(\mathbf{x},t) = \hat{\mathbf{A}}(\mathbf{x},\omega)\mathrm{e}^{-\mathrm{i}\omega t} + \text{c.c.}$, and analogously for current and charge density, field strengths, and inductions. The Fourier amplitudes of Proca fields with negative mass-square solve the tachyonic Maxwell equations [22]

$$\begin{aligned} &\operatorname{rot}\hat{\mathbf{H}} + \mathrm{i}\omega\hat{\mathbf{D}} = \hat{\mathbf{j}} + m_\mathrm{t}^2\hat{\mathbf{C}}, \qquad \operatorname{div}\hat{\mathbf{D}} = \hat{\rho} - m_\mathrm{t}^2\hat{C}_0, \\ &\operatorname{rot}\hat{\mathbf{E}} - \mathrm{i}\omega\hat{\mathbf{B}} = 0, \qquad \operatorname{div}\hat{\mathbf{B}} = 0, \end{aligned} \tag{2.1}$$

where $m_\mathrm{t} > 0$ is the tachyon mass. The mass-square refers to the radiation field rather than the current, in contrast to traditional theories based on superluminal source particles emitting electromagnetic radiation [4–6]. The constitutive equations read [23–26]

$$\begin{aligned} &\hat{\mathbf{D}}(\mathbf{x},\omega) = \varepsilon(\omega)\hat{\mathbf{E}}(\mathbf{x},\omega), \qquad \hat{\mathbf{B}}(\mathbf{x},\omega) = \mu(\omega)\hat{\mathbf{H}}(\mathbf{x},\omega), \\ &\hat{\mathbf{A}}(\omega) = \mu_0(\omega)\hat{\mathbf{C}}(\omega), \qquad \hat{C}_0(\omega) = \varepsilon_0(\omega)\hat{A}_0(\omega). \end{aligned} \tag{2.2}$$

The field equations (2.1) are based on the Lagrangian

$$L_\mathrm{P} = \frac{1}{2}(\mathbf{ED} - \mathbf{BH}) + \frac{1}{2}m_\mathrm{t}^2(\mathbf{AC} - A_0C_0) + \mathbf{Aj} + A_0\rho. \tag{2.3}$$

The mass term is added with a positive sign, so that $m_\mathrm{t}^2 > 0$ is the negative mass-square of the radiation field. The potentials $(\hat{A}_0, \hat{\mathbf{A}})$ and field strengths $\hat{\mathbf{E}}$ and $\hat{\mathbf{B}}$ are primary fields, whereas the inductive potentials $(\hat{C}_0, \hat{\mathbf{C}})$ and inductions $\hat{\mathbf{D}}$ and $\hat{\mathbf{H}}$ are connected to the primary fields by frequency-dependent dielectric $(\varepsilon_0, \varepsilon)$ and magnetic (μ_0, μ) permeabilities. We may use primary fields instead of inductions, writing the inhomogeneous equations in (2.1) as

$$\begin{aligned} &\operatorname{rot}\hat{\mathbf{B}} + \mathrm{i}\omega\varepsilon\mu\hat{\mathbf{E}} = \mu\hat{\mathbf{j}} + m_\mathrm{t}^2\frac{\mu}{\mu_0}\hat{\mathbf{A}}, \\ &\operatorname{div}\hat{\mathbf{E}} = \frac{1}{\varepsilon}\hat{\rho} - m_\mathrm{t}^2\frac{\varepsilon_0}{\varepsilon}\hat{A}_0. \end{aligned} \tag{2.4}$$

The field strengths are related to the tachyonic potentials by $\hat{\mathbf{E}} = \mathrm{i}\omega\hat{\mathbf{A}} + \nabla\hat{A}_0$ and $\hat{\mathbf{B}} = \operatorname{rot}\hat{\mathbf{A}}$. We take the divergence of the first equation in (2.4), and substitute the second, to obtain

$$\mu_0(\mathrm{i}\omega\hat{\rho} - \operatorname{div}\hat{\mathbf{j}}) = m_\mathrm{t}^2(\operatorname{div}\hat{\mathbf{A}} + \mathrm{i}\omega\varepsilon_0\mu_0\hat{A}_0). \tag{2.5}$$

Current conservation, $\mathrm{i}\omega\hat{\rho} = \operatorname{div}\hat{\mathbf{j}}$, implies the Lorentz condition $\operatorname{div}\hat{\mathbf{A}} + \mathrm{i}\omega\varepsilon_0\mu_0\hat{A}_0 = 0$ or $\mathrm{i}\omega\hat{C}_0 + \operatorname{div}\hat{\mathbf{C}} = 0$. The permeabilities ε_0 and μ_0 define the inductive potentials, and are not to be confused with vacuum permeabilities; we use the Heaviside–Lorentz system, so that $\varepsilon = \varepsilon_0 = 1$ and $\mu = \mu_0 = 1$ in vacuum. The potentials $(A_0, \mathbf{A})$ are determined by the current and field strengths, and there is no gauge freedom owing to the tachyon mass, as the inductive potentials $(C_0, \mathbf{C})$ appear explicitly in the tachyonic Maxwell equations. By applying the rotor to the rotor equations in (2.1) and (2.4), we obtain wave equations for the field strengths,

$$\begin{aligned} &\left(\Delta + \varepsilon\mu\omega^2 + \frac{\mu}{\mu_0}m_\mathrm{t}^2\right)\hat{\mathbf{E}} + \left(\frac{\varepsilon}{\varepsilon_0}\frac{\mu}{\mu_0} - 1\right)\nabla\operatorname{div}\hat{\mathbf{E}} \\ &\quad = -\mathrm{i}\omega\mu\hat{\mathbf{j}} + \frac{\mu}{\mu_0}\frac{1}{\varepsilon_0}\nabla\hat{\rho}, \\ &\left(\Delta + \varepsilon\mu\omega^2 + \frac{\mu}{\mu_0}m_\mathrm{t}^2\right)\hat{\mathbf{B}} = -\mu\operatorname{rot}\hat{\mathbf{j}}. \end{aligned} \tag{2.6}$$

The above equations stay valid without alterations for polychromatic fields, if Fourier transforms are used,

$$\begin{aligned} &\mathbf{A}(\mathbf{x},t) = \frac{1}{2\pi}\int_0^\infty \left(\hat{\mathbf{A}}(\mathbf{x},\omega)\mathrm{e}^{-\mathrm{i}\omega t} + \text{c.c.}\right)\mathrm{d}\omega, \\ &\hat{\mathbf{A}}(\mathbf{x},\omega) = \int_{-\infty}^{+\infty}\mathbf{A}(\mathbf{x},t)\mathrm{e}^{\mathrm{i}\omega t}\,\mathrm{d}t, \end{aligned} \tag{2.7}$$

and analogously for the current and charge densities, field strengths, and inductions. The Fourier modes are continued to negative frequencies via $\hat{\mathbf{A}}^*(\mathbf{x},\omega)=\hat{\mathbf{A}}(\mathbf{x},-\omega)$ and $\varepsilon^*(\omega)=\varepsilon(-\omega)$, so that we can drop the conjugated terms in (2.7) and extend the lower integration boundary to $-\infty$.

3 Superluminal radiation: polarization, energy, and flux

3.1 Transversal and longitudinal modes in a permeable space

We study plane-wave solutions of the field equations with vanishing charge and current distributions. In the Fourier ansatz defined before (2.1), we put $\hat{\mathbf{A}}(\mathbf{x},\omega)=\mathbf{A}(\mathbf{k})\mathrm{e}^{\mathrm{i}\mathbf{k}\mathbf{x}}$, $\hat{A}_0=A_0(\mathbf{k})\mathrm{e}^{\mathrm{i}\mathbf{k}\mathbf{x}}$, $\hat{\mathbf{E}}=\mathbf{E}(\mathbf{k})\mathrm{e}^{\mathrm{i}\mathbf{k}\mathbf{x}}$, $\hat{\mathbf{B}}=\mathbf{B}(\mathbf{k})\mathrm{e}^{\mathrm{i}\mathbf{k}\mathbf{x}}$, and calculate the dispersion relations and the amplitudes $A_0(\mathbf{k})$, $\mathbf{E}(\mathbf{k})$, and $\mathbf{B}(\mathbf{k})$ in terms of a prescribed vector potential $\mathbf{A}(\mathbf{k})$. To this end, we define $\mathbf{k}=k(\omega)\mathbf{k}_0$, where the wave number $k(\omega)$ can be complex and $\mathbf{k}_0$ is a constant unit vector, also complex in general. (A complex unit vector satisfies $\mathbf{k}_0^2=1$; the scalar product $\mathbf{k}^2$ is not to be confused with the norm $|\mathbf{k}|^2=\mathbf{k}\mathbf{k}^*$.) We start with an arbitrary amplitude $\mathbf{A}(\mathbf{k})$, and use the Lorentz condition to obtain

$$A_0(\mathbf{k})=-\frac{k(\omega)}{\varepsilon_0\mu_0\omega}\mathbf{k}_0\mathbf{A}(\mathbf{k}). \tag{3.1}$$

The potential representation of the tachyonic field strengths gives the amplitudes $\mathbf{E}(\mathbf{k})$ and $\mathbf{B}(\mathbf{k})$ in terms of $\mathbf{A}(\mathbf{k})$ and $\mathbf{k}=k\mathbf{k}_0$,

$$\begin{aligned}&\mathbf{E}(\mathbf{k})=\mathrm{i}\omega\biggl(\mathbf{A}-\frac{k^2}{\varepsilon_0\mu_0\omega^2}(\mathbf{A}\mathbf{k}_0)\mathbf{k}_0\biggr),\\&\mathbf{B}(\mathbf{k})=\mathrm{i}k\mathbf{k}_0\times\mathbf{A}.\end{aligned} \tag{3.2}$$

The homogeneous Maxwell equations in (2.1) are solved by this ansatz, and the inhomogeneous equations (2.4) (with charge and current put to zero) read

$$\begin{aligned}&\operatorname{rot}\hat{\mathbf{B}}=k^2\bigl(\hat{\mathbf{A}}-(\hat{\mathbf{A}}\mathbf{k}_0)\mathbf{k}_0\bigr),\\&\operatorname{div}\hat{\mathbf{E}}=\frac{k}{\varepsilon_0\mu_0\omega}\bigl(k^2-\varepsilon_0\mu_0\omega^2\bigr)\hat{\mathbf{A}}\mathbf{k}_0.\end{aligned} \tag{3.3}$$

The transversality condition is $\hat{\mathbf{A}}\mathbf{k}_0=0$, so that the divergence equation in (3.3) is satisfied, and the rotor equation requires the transversal dispersion relation

$$k_\mathrm{T}^2=\varepsilon\mu\omega^2+m_\mathrm{t}^2\mu/\mu_0. \tag{3.4}$$

In this way, we find the set of transversal modes as

$$\begin{aligned}&\mathbf{k}_0\hat{\mathbf{A}}^\mathrm{T}=0,\qquad \hat{A}_0^\mathrm{T}=0,\\&\hat{\mathbf{E}}^\mathrm{T}=\mathrm{i}\omega\hat{\mathbf{A}}^\mathrm{T},\qquad \hat{\mathbf{B}}^\mathrm{T}=\mathrm{i}k_\mathrm{T}\mathbf{k}_0\times\hat{\mathbf{A}}^\mathrm{T}.\end{aligned} \tag{3.5}$$

In terms of inductions,

$$\begin{aligned}&\mathbf{k}_0\hat{\mathbf{C}}^\mathrm{T}=0,\qquad \hat{C}_0^\mathrm{T}=0,\qquad \hat{\mathbf{D}}^\mathrm{T}=\mathrm{i}\varepsilon\mu_0\omega\hat{\mathbf{C}}^\mathrm{T},\\&\hat{\mathbf{H}}^\mathrm{T}=\mathrm{i}\frac{\mu_0}{\mu}k_\mathrm{T}\mathbf{k}_0\times\hat{\mathbf{C}}^\mathrm{T},\end{aligned} \tag{3.6}$$

and we also note the inversions

$$\hat{\mathbf{A}}^\mathrm{T}=\frac{\mathrm{i}}{k_\mathrm{T}}\mathbf{k}_0\times\hat{\mathbf{B}}^\mathrm{T},\qquad \hat{\mathbf{C}}^\mathrm{T}=\frac{\mathrm{i}}{k_\mathrm{T}}\frac{\mu}{\mu_0}\mathbf{k}_0\times\hat{\mathbf{H}}^\mathrm{T}. \tag{3.7}$$

Longitudinal polarization occurs if the product $\hat{\mathbf{A}}\mathbf{k}_0$ does not vanish [27]. The divergence equation in (3.3) implies the longitudinal dispersion relation

$$k_\mathrm{L}^2=\varepsilon_0\mu_0\omega^2+m_\mathrm{t}^2\varepsilon_0/\varepsilon, \tag{3.8}$$

and the rotor equation reduces to $\hat{\mathbf{A}}=(\hat{\mathbf{A}}\mathbf{k}_0)\mathbf{k}_0$. Hence, if $\hat{\mathbf{A}}$ and $\mathbf{k}_0$ are not orthogonal, the modes must be longitudinal,

$$\begin{aligned}&\hat{\mathbf{A}}^\mathrm{L}=\bigl(\hat{\mathbf{A}}^\mathrm{L}\mathbf{k}_0\bigr)\mathbf{k}_0,\qquad \hat{A}_0^\mathrm{L}=-\frac{k_\mathrm{L}}{\varepsilon_0\mu_0\omega}\mathbf{k}_0\hat{\mathbf{A}}^\mathrm{L},\\&\hat{\mathbf{E}}^\mathrm{L}=\frac{m_\mathrm{t}^2}{\mathrm{i}\varepsilon\mu_0\omega}\hat{\mathbf{A}}^\mathrm{L},\qquad \hat{\mathbf{B}}^\mathrm{L}=0.\end{aligned} \tag{3.9}$$

The associated longitudinal inductions are

$$\begin{aligned}&\hat{\mathbf{C}}^\mathrm{L}=\bigl(\hat{\mathbf{C}}^\mathrm{L}\mathbf{k}_0\bigr)\mathbf{k}_0,\qquad \hat{C}_0^\mathrm{L}=-\frac{k_\mathrm{L}}{\omega}\mathbf{k}_0\hat{\mathbf{C}}^\mathrm{L},\\&\hat{\mathbf{D}}^\mathrm{L}=\frac{m_\mathrm{t}^2}{\mathrm{i}\omega}\hat{\mathbf{C}}^\mathrm{L},\qquad \hat{\mathbf{H}}^\mathrm{L}=0.\end{aligned} \tag{3.10}$$

Longitudinal modes thus imply wave propagation without magnetic component. Inversely,

$$\hat{A}_0^\mathrm{L}=\frac{1}{\mathrm{i}}\frac{\varepsilon}{\varepsilon_0}\frac{k_\mathrm{L}}{m_\mathrm{t}^2}\mathbf{k}_0\hat{\mathbf{E}}^\mathrm{L},\qquad \hat{C}_0^\mathrm{L}=\frac{1}{\mathrm{i}}\frac{k_\mathrm{L}}{m_\mathrm{t}^2}\mathbf{k}_0\hat{\mathbf{D}}^\mathrm{L}. \tag{3.11}$$

The transversal and longitudinal dispersion relations coincide for $\varepsilon_0=\varepsilon$ and $\mu_0=\mu$. In the case of homogeneous plane waves, real $\mathbf{k}_0$ that is, the waves propagate in the prescribed direction $\mathbf{k}_0$ if the roots of (3.4) and (3.8) defining the wave numbers $k_{\mathrm{T,L}}$ are taken with positive real part. If we put $\mu_0=\mu$ and $\varepsilon_0=\varepsilon=1/\mu$, the permeabilities drop out in the dispersion relations. In the field equations, they can be absorbed in the charge and current densities by way of a frequency-dependent rescaling $\propto\mu(\omega)$ of the coupling constant q_t, provided that μ is real; this will be discussed in Sect. 4. The tachyonic fine-structure constant then scales as $\alpha_\mathrm{q}=q_\mathrm{t}^2\mu^2(\omega)/(4\pi)$, cf. (4.7), and the time averaged flux vectors (3.21) and energy densities (3.24) conformally scale $\propto 1/\mu$.

3.2 Superluminal energy transport in a dispersive and absorptive medium

To find the energy flux in a dispersive medium, we start with the tachyonic Maxwell equations in real time,

$$\begin{aligned} &\operatorname{div}\mathbf{B}(\mathbf{x},t)=0, \qquad \operatorname{rot}\mathbf{E}+\partial\mathbf{B}/\partial t=0,\\ &\operatorname{div}\mathbf{D}=\rho-m_{\mathrm{t}}^2C_0, \qquad \operatorname{rot}\mathbf{H}-\partial\mathbf{D}/\partial t=\mathbf{j}+m_{\mathrm{t}}^2\mathbf{C}. \end{aligned} \tag{3.12}$$

The field strengths are related to the vector potential by $\mathbf{E}=\nabla A_0-\partial\mathbf{A}/\partial t$ and $\mathbf{B}=\operatorname{rot}\mathbf{A}$. The Lorentz condition, $\operatorname{div}\mathbf{C}-\partial C_0/\partial t=0$, follows from the field equations and current conservation, $\operatorname{div}\mathbf{j}+\partial\rho/\partial t=0$, cf. (2.5). Defining the tachyonic flux vector as

$$\mathbf{S}=\mathbf{E}\times\mathbf{H}+m_{\mathrm{t}}^2A_0\mathbf{C}, \tag{3.13}$$

we find, by means of the field equations (3.12), the identity [28]

$$\operatorname{div}\mathbf{S}+\mathbf{E}\frac{\partial\mathbf{D}}{\partial t}+\mathbf{H}\frac{\partial\mathbf{B}}{\partial t}-m_{\mathrm{t}}^2\left(A_0\frac{\partial C_0}{\partial t}+\mathbf{C}\frac{\partial\mathbf{A}}{\partial t}\right)=-\mathbf{j}\mathbf{E}. \tag{3.14}$$

First, we consider constant (i.e. frequency-independent) real permeabilities, so that the material equations read $\mathbf{D}(\mathbf{x},t)=\varepsilon\mathbf{E}(\mathbf{x},t)$, $\mathbf{B}=\mu\mathbf{H}$, $\mathbf{A}=\mu_0\mathbf{C}$, and $C_0=\varepsilon_0A_0$, cf. (2.2). Based on the field equations and current conservation, we obtain the conservation law $\operatorname{div}\mathbf{S}+\partial\rho_{\mathrm{E}}/\partial t=-\mathbf{E}\mathbf{j}$, with the flux vector (3.13) and energy density

$$\rho_{\mathrm{E}}=\frac{1}{2}(\mathbf{E}\mathbf{D}+\mathbf{B}\mathbf{H})-\frac{1}{2}m_{\mathrm{t}}^2(A_0C_0+\mathbf{A}\mathbf{C}). \tag{3.15}$$

To find the energy density in a dispersive medium with frequency-dependent permeabilities, we have to extract the energy density from the incomplete time derivative $\rho_{\mathrm{E},t}=(\mathbf{E}\mathbf{D}_{,t}+\mathbf{B}_{,t}\mathbf{H})-m_{\mathrm{t}}^2(A_0C_{0,t}+\mathbf{A}_{,t}\mathbf{C})$, which replaces $\partial\rho_{\mathrm{E}}/\partial t$ in the above conservation law. Real permeabilities will be assumed when discussing energy averages, but the flux vectors (3.19) stated below also apply in an absorptive medium.

We start with a plane wave $\mathbf{E}(\omega,t)=\hat{\mathbf{E}}\mathrm{e}^{-\mathrm{i}\omega t}+\text{c.c.}$, and consider the symmetrized product $\mathbf{E}(\omega,t)\partial\mathbf{D}(\omega',t)/\partial t$ with the constitutive relation $\hat{\mathbf{D}}=\varepsilon(\omega)\hat{\mathbf{E}}$. Expanding in ascending powers of $\omega'-\omega$ except for the phase, we obtain, in the limit $\omega'\to\omega$ [23],

$$\begin{aligned} &\frac{1}{2}\left(\mathbf{E}(\omega,t)\frac{\partial}{\partial t}\mathbf{D}(\omega',t)+(\omega'\leftrightarrow\omega)\right)=\frac{\partial}{\partial t}\rho_{ED},\\ &\rho_{ED}=\frac{1}{2}\frac{\mathrm{d}\varepsilon(\omega)\omega}{\mathrm{d}\omega}\hat{\mathbf{E}}(\omega)\hat{\mathbf{E}}^*(\omega)+\frac{1}{2}\varepsilon(\omega)\hat{\mathbf{E}}^2(\omega)\mathrm{e}^{-2\mathrm{i}\omega t}+\text{c.c.} \end{aligned} \tag{3.16}$$

The time averaged ρ_{ED} at $\omega'=\omega$ is $\langle\rho_{ED}\rangle=\hat{\mathbf{E}}\hat{\mathbf{E}}^*\,\mathrm{d}(\omega\varepsilon)/\mathrm{d}\omega$, replacing the term $\mathbf{E}\mathbf{D}/2$ in energy density (3.15); terms depending on $\exp(\pm2\mathrm{i}\omega t)$ drop out if averaged over the period $2\pi/\omega$. The remaining three pairs in (3.15) can be treated on equal footing: The averaged $\mathbf{H}\partial\mathbf{B}/\partial t$ contributes the term $\langle\rho_{HB}\rangle=\hat{\mathbf{H}}\hat{\mathbf{H}}^*(\omega\mu)'$ to the energy density, the averaging of $A_0\partial C_0/\partial t$ amounts to $\langle\rho_{A_0C_0}\rangle=\hat{A}_0\hat{A}_0^*(\omega\varepsilon_0)'$, and $\mathbf{C}\partial\mathbf{A}/\partial t$ gives $\langle\rho_{CA}\rangle=\hat{\mathbf{C}}\hat{\mathbf{C}}^*(\omega\mu_0)'$. These three averages replace $\mathbf{B}\mathbf{H}/2$, $A_0C_0/2$, and $\mathbf{A}\mathbf{C}/2$, respectively. Accordingly, the energy carried by a superluminal mode $\mathbf{A}(\omega,t)=\hat{\mathbf{A}}\mathrm{e}^{-\mathrm{i}\omega t}+\text{c.c.}$ in a dispersive medium reads

$$\begin{aligned} \langle\rho_{\mathrm{E}}\rangle=\;&\hat{\mathbf{E}}\hat{\mathbf{E}}^*(\omega\varepsilon)'+\hat{\mathbf{H}}\hat{\mathbf{H}}^*(\omega\mu)'-m_{\mathrm{t}}^2\hat{A}_0\hat{A}_0^*(\omega\varepsilon_0)'\\ &-m_{\mathrm{t}}^2\hat{\mathbf{C}}\hat{\mathbf{C}}^*(\omega\mu_0)'. \end{aligned} \tag{3.17}$$

The tachyonic flux vector is obtained by substituting the Fourier modes into the Poynting vector (3.13) and performing a time average [28],

$$\langle\mathbf{S}\rangle=\frac{1}{\mu^*}\hat{\mathbf{E}}\times\hat{\mathbf{B}}^*+\frac{m_{\mathrm{t}}^2}{\mu_0^*}\hat{A}_0\hat{\mathbf{A}}^*+\text{c.c.} \tag{3.18}$$

This flux vector also applies in a dissipative medium; the nonconservation of energy due to absorption is manifested by an exponential damping factor in the Fourier amplitudes, cf. (3.26) below.

We consider homogeneous plane-wave solutions propagating in the direction of the real unit vector $\mathbf{k}_0$. The transversal/longitudinal energy and flux components $\langle\rho_{\mathrm{E}}^{\mathrm{T,L}}\rangle$ and $\langle\mathbf{S}^{\mathrm{T,L}}\rangle$ are found by replacing the Fourier amplitudes in (3.17) and (3.18) by the respective polarized components (3.5) and (3.9),

$$\begin{aligned} \langle\mathbf{S}^{\mathrm{T}}\rangle&=\frac{\mu^*k_{\mathrm{T}}+\mu k_{\mathrm{T}}^*}{|\mu|^2}\omega\left|\hat{\mathbf{A}}^{\mathrm{T}}\right|^2\mathbf{k}_0,\\ \langle\mathbf{S}^{\mathrm{L}}\rangle&=\frac{\varepsilon_0^*k_{\mathrm{L}}+\varepsilon_0k_{\mathrm{L}}^*}{|\mu_0|^2|\varepsilon_0|^2}\frac{m_{\mathrm{t}}^2}{\omega}\left|\hat{\mathbf{A}}^{\mathrm{L}}\right|^2\mathbf{k}_0. \end{aligned} \tag{3.19}$$

These flux vectors are quite general, applying to frequency-dependent complex permeabilities (generating complex wave numbers $k_{\mathrm{T,L}}$) and homogeneous modes (whose wave vector is a complex multiple of a real unit vector $\mathbf{k}_0$). In the absence of absorption, the associated transversal and longitudinal tachyonic energy densities (3.17) are assembled with the modes derived in Sect. 3.1,

$$\begin{aligned} \langle\rho^{\mathrm{T}}\rangle&=\left|\hat{\mathbf{A}}^{\mathrm{T}}\right|^2\left[\omega^2(\omega\varepsilon)'+k_{\mathrm{T}}^2\frac{(\omega\mu)'}{\mu^2}-m_{\mathrm{t}}^2\frac{(\omega\mu_0)'}{\mu_0^2}\right],\\ \langle\rho^{\mathrm{L}}\rangle&=\frac{1}{\mu_0^2}\frac{m_{\mathrm{t}}^2}{\omega^2}\left|\hat{\mathbf{A}}^{\mathrm{L}}\right|^2\left[\omega^2(\omega\mu_0)'+k_{\mathrm{L}}^2\frac{(\omega\varepsilon_0)'}{\varepsilon_0^2}-m_{\mathrm{t}}^2\frac{(\omega\varepsilon)'}{\varepsilon^2}\right], \end{aligned} \tag{3.20}$$

with real permeabilities $(\varepsilon,\varepsilon_0,\mu_0,\mu)$. The energy carried by a superluminal mode propagates with speed $\mathbf{v}_{\mathrm{T,L}}=\langle\mathbf{S}^{\mathrm{T,L}}\rangle/\langle\rho^{\mathrm{T,L}}\rangle$, cf. Sects. 3.3 and 5.3.

3.3 Transversal and longitudinal group velocity and attenuation length of tachyonic modes

In the case of real and frequency-independent permeabilities, we find the transversal and longitudinal flux components as, cf. (3.19),

$$\langle \mathbf{S}^{\mathrm{T}} \rangle = \frac{2k_{\mathrm{T}}}{\mu}\omega \big|\hat{\mathbf{A}}^{\mathrm{T}}\big|^2 \mathbf{k}_0, \qquad \langle \mathbf{S}^{\mathrm{L}} \rangle = \frac{2k_{\mathrm{L}}}{\mu_0^2 \varepsilon_0}\frac{m_{\mathrm{t}}^2}{\omega}\big|\hat{\mathbf{A}}^{\mathrm{L}}\big|^2 \mathbf{k}_0. \quad (3.21)$$

The corresponding tachyonic energy densities read, cf. (3.20),

$$\langle \rho^{\mathrm{T}} \rangle = 2\varepsilon\omega^2 \big|\hat{\mathbf{A}}^{\mathrm{T}}\big|^2, \qquad \langle \rho^{\mathrm{L}} \rangle = 2\frac{m_{\mathrm{t}}^2}{\mu_0}\big|\hat{\mathbf{A}}^{\mathrm{L}}\big|^2. \quad (3.22)$$

We note the transversal and longitudinal group velocities

$$\frac{1}{\upsilon_{\mathrm{T}}} = \frac{\mathrm{d}k_{\mathrm{T}}}{\mathrm{d}\omega} = \varepsilon\mu\frac{\omega}{k_{\mathrm{T}}}, \qquad \frac{1}{\upsilon_{\mathrm{L}}} = \frac{\mathrm{d}k_{\mathrm{L}}}{\mathrm{d}\omega} = \varepsilon_0\mu_0\frac{\omega}{k_{\mathrm{L}}}, \quad (3.23)$$

to be compared to the phase velocity $\upsilon_{\mathrm{ph}} = \omega/k_{\mathrm{T,L}}$ in the medium. We may thus identify $\upsilon_{\mathrm{T,L}}\mathbf{k}_0$ with the speed of energy transfer $\mathbf{v}_{\mathrm{T,L}}$ as defined after (3.20). If $\varepsilon = \mu = 1$ and $\varepsilon_0 = \mu_0 = 1$, the transversal and longitudinal velocities coincide, so that $\omega = m_{\mathrm{t}}\gamma_{\mathrm{t}}$, with the tachyonic Lorentz factor $\gamma_{\mathrm{t}} = (\upsilon_{\mathrm{T,L}}^2 - 1)^{-1/2}$.

We study a dispersive transparent medium, where the permeabilities are real and frequency dependent, so that $k_{\mathrm{T,L}}^2 > 0$, cf. (3.4) and (3.8). The permeabilities may even be negative, if we restrict to a frequency range admitting positive squared wave numbers [17]. As in the previous case, we find the identity $\langle \mathbf{S}^{\mathrm{T,L}} \rangle = \mathbf{k}_0 \langle \rho^{\mathrm{T,L}} \rangle \,\mathrm{d}\omega/\mathrm{d}k_{\mathrm{T,L}}$, which allows us to identify the group velocity $\mathbf{k}_0\,\mathrm{d}\omega/\mathrm{d}k_{\mathrm{T,L}}$ as the speed of energy transfer $\langle \mathbf{S}^{\mathrm{T,L}} \rangle / \langle \rho^{\mathrm{T,L}} \rangle$. The flux vectors $\langle \mathbf{S}^{\mathrm{T,L}} \rangle$ in (3.21) remain valid for frequency-dependent real permeabilities, and the energy densities read

$$\langle \rho^{\mathrm{T}} \rangle = \frac{\omega}{\mu}\frac{\mathrm{d}k_{\mathrm{T}}^2}{\mathrm{d}\omega}\big|\hat{\mathbf{A}}^{\mathrm{T}}\big|^2, \qquad \langle \rho^{\mathrm{L}} \rangle = \frac{1}{\mu_0^2\varepsilon_0}\frac{m_{\mathrm{t}}^2}{\omega}\frac{\mathrm{d}k_{\mathrm{L}}^2}{\mathrm{d}\omega}\big|\hat{\mathbf{A}}^{\mathrm{L}}\big|^2, \quad (3.24)$$

derived from (3.20) by expressing the real dielectric permeability ε in terms of k_{T}^2 or k_{L}^2 via the dispersion relations. More explicitly, the energy densities associated with the flux vectors $\langle \mathbf{S}^{\mathrm{T,L}} \rangle$ in (3.21) read, according to (3.20),

$$\begin{aligned}
\langle \rho^{\mathrm{T}} \rangle &= \big|\hat{\mathbf{A}}^{\mathrm{T}}\big|^2 \bigg[\varepsilon\omega^2\bigg(2 + \frac{\varepsilon'}{\varepsilon}\omega + \frac{\mu'}{\mu}\omega\bigg) + \frac{m_{\mathrm{t}}^2}{\mu_0}\omega\bigg(\frac{\mu'}{\mu} - \frac{\mu_0'}{\mu_0}\bigg)\bigg], \\
\langle \rho^{\mathrm{L}} \rangle &= \frac{1}{\mu_0^2}\frac{m_{\mathrm{t}}^2}{\omega^2}\big|\hat{\mathbf{A}}^{\mathrm{L}}\big|^2 \bigg[\mu_0\omega^2\bigg(2 + \frac{\mu_0'}{\mu_0}\omega + \frac{\varepsilon_0'}{\varepsilon_0}\omega\bigg) \\
&\quad + \frac{m_{\mathrm{t}}^2}{\varepsilon}\omega\bigg(\frac{\varepsilon_0'}{\varepsilon_0} - \frac{\varepsilon'}{\varepsilon}\bigg)\bigg].
\end{aligned} \quad (3.25)$$

They apply in a nonabsorptive medium.

In a dissipative medium with frequency-dependent complex permeabilities, we employ the flux densities (3.19), applicable to homogeneous plane waves (real $\mathbf{k}_0$). Writing the wave number $k_{\mathrm{T,L}}$ as $k = k_{\mathrm{Re}} + \mathrm{i}k_{\mathrm{Im}}$ with $k_{\mathrm{Re}} > 0$, we obtain the squared amplitudes in (3.19) as

$$\big|\hat{\mathbf{A}}^{\mathrm{T,L}}\big|^2 = \big|\mathbf{A}^{\mathrm{T,L}}(\mathbf{k})\big|^2 \exp(-2k_{\mathrm{Im}}\mathbf{k}_0\mathbf{x}). \quad (3.26)$$

Thus, $\mathrm{Im}(k_{\mathrm{T,L}}) \geq 0$ is required for damping, and $\delta := 1/k_{\mathrm{Im}}$ is the tachyonic attenuation length or skin depth of the absorptive medium. The above formalism is based on real frequencies and complex wave numbers, convenient to derive penetration depths. In Ref. [28], we used complex frequencies and real wave vectors to calculate decay times. One may switch to complex frequencies by analytically continuing the dispersion relations, the imaginary part of ω being determined by $\mathrm{Im}(k) = 0$.

4 Proca fields with negative mass-square coupled to nonlocal currents

The tachyonic radiation field in vacuum satisfies the Proca equation $(\partial^\nu\partial_\nu + m_{\mathrm{t}}^2)A_\mu = -j_\mu$, subject to the Lorentz condition $A^\mu{}_{,\mu} = 0$ [2, 7]. m_{t} is the mass of the real superluminal Proca field A_μ, and $j^\mu = (\rho, \mathbf{j})$ the conserved subluminal electron current, cf. Sect. 2. In the Proca equation, the mass term is added with a positive sign, so that $m_{\mathrm{t}}^2 > 0$ is the negative mass-square of the radiation field, and the sign convention for the metric is $\mathrm{diag}(-1, 1, 1, 1)$. Fourier transforms are denoted by a hat, $\mathbf{A}(\mathbf{x}, t) = (2\pi)^{-1}\int_{-\infty}^{+\infty}\hat{\mathbf{A}}(\mathbf{x}, \omega)\mathrm{e}^{-\mathrm{i}\omega t}\,\mathrm{d}\omega$, cf. (2.7). In Fourier space, the Proca equation can be written as

$$\begin{aligned}
\big(\Delta + k^2\big)\hat{A}_0(\mathbf{x}, \omega) &= \hat{\rho}(\mathbf{x}, \omega), \\
\big(\Delta + k^2\big)\hat{\mathbf{A}}(\mathbf{x}, \omega) &= -\hat{\mathbf{j}}(\mathbf{x}, \omega),
\end{aligned} \quad (4.1)$$

where $k = \sqrt{\omega^2 + m_{\mathrm{t}}^2}$ is the wave number of the tachyonic modes. Current conservation $\mathrm{i}\omega\hat{\rho} = \mathrm{div}\,\hat{\mathbf{j}}$ implies the Lorentz condition $\mathrm{i}\omega\hat{A}_0 + \mathrm{div}\,\hat{\mathbf{A}} = 0$, cf. (2.5). The vacuum field equations in Fourier space are stated in (2.1) and (2.4), with $\varepsilon = \varepsilon_0 = 1$ and $\mu = \mu_0 = 1$. The whole-space Green's function inverting the field equations (4.1) reads

$$\begin{aligned}
G(\mathbf{x}, \mathbf{x}_0; \omega) &= \frac{1}{4\pi}\frac{\mathrm{e}^{\mathrm{i}k(\omega)|\mathbf{x}-\mathbf{x}_0|}}{|\mathbf{x} - \mathbf{x}_0|}, \\
\big(\Delta + k^2\big)G(\mathbf{x}, \mathbf{x}_0; \omega) &= -\delta(\mathbf{x} - \mathbf{x}_0),
\end{aligned} \quad (4.2)$$

with $k(\omega)$ as in (4.1), so that the tachyon potential is calculated as

$$\begin{aligned}
&\big(\hat{A}_0(\mathbf{x}, \omega), \hat{\mathbf{A}}(\mathbf{x}, \omega)\big) \\
&\quad = \int G(\mathbf{x}, \mathbf{x}'; \omega)\big(-\hat{\rho}(\mathbf{x}', \omega), \hat{\mathbf{j}}(\mathbf{x}', \omega)\big)\,\mathrm{d}^3x'.
\end{aligned} \quad (4.3)$$

The singular charge and current densities of a classical subluminal point particle with trajectory $\mathbf{x}_0(t)$ read $\rho(\mathbf{x},t) = q_\mathrm{t}\delta(\mathbf{x}-\mathbf{x}_0(t))$ and $\mathbf{j}(\mathbf{x},t) = \dot{\mathbf{x}}_0(t)\rho(\mathbf{x},t)$, where q_t is the tachyonic charge, defining the fine-structure constant $\alpha_\mathrm{t} = q_\mathrm{t}^2/(4\pi\hbar c)$ in the Heaviside-Lorentz system. In the field equations (4.1), we use the Fourier amplitudes

$$\begin{aligned}\hat{\rho}(\mathbf{x},\omega) &= q_\mathrm{t}\int_{-\infty}^{+\infty}\delta\big(\mathbf{x}-\mathbf{x}_0(t)\big)\mathrm{e}^{\mathrm{i}\omega t}\,\mathrm{d}t,\\ \hat{\mathbf{j}}(\mathbf{x},\omega) &= q_\mathrm{t}\int_{-\infty}^{+\infty}\dot{\mathbf{x}}_0(t)\delta\big(\mathbf{x}-\mathbf{x}_0(t)\big)\mathrm{e}^{\mathrm{i}\omega t}\,\mathrm{d}t.\end{aligned} \tag{4.4}$$

Alternatively, we may consider a Dirac current $j^\mu = (\rho,\mathbf{j}) = -q_\mathrm{t}\bar{\psi}\gamma^\mu\psi$, and replace the classical amplitudes (4.4) by spinorial matrix elements $\hat{\rho}_{mn}(\mathbf{x})$ and $\hat{\mathbf{j}}_{mn}(\mathbf{x})$ [20, 29].

The nonlocal coupling of the superluminal radiation field to the electron current is effected by a frequency-dependent coupling constant $q(\omega)$, which replaces q_t in the Fourier amplitudes (4.4) and the corresponding matrix elements [3]. $q(\omega)$ scales with a power of the tachyonic velocity,

$$q(\omega) = q_\mathrm{t}\upsilon_\mathrm{t}^\sigma, \qquad \upsilon_\mathrm{t}(\omega) = k/\omega = \sqrt{1+m_\mathrm{t}^2/\omega^2}, \tag{4.5}$$

so that q_t is recovered in the high-frequency limit $q(\omega\to\infty) = q_\mathrm{t}$. The frequency and wave number of the tachyonic modes can as well be parametrized by their superluminal velocity $\upsilon_\mathrm{t} > 1$,

$$\omega = \frac{m_\mathrm{t}}{\sqrt{\upsilon_\mathrm{t}^2-1}}, \qquad k(\omega) = \frac{m_\mathrm{t}\upsilon_\mathrm{t}}{\sqrt{\upsilon_\mathrm{t}^2-1}}. \tag{4.6}$$

As mentioned, the sign conventions in the wave equation are such that the tachyon mass m_t is a positive quantity. The varying tachyonic fine-structure constant reads

$$\begin{aligned}\alpha_\mathrm{q}(\omega) &= \frac{q^2(\omega)}{4\pi\hbar c} = \alpha_\mathrm{t}\hat{\Omega}^2(\omega),\\ \hat{\Omega}(\omega) &= \upsilon_\mathrm{t}^\sigma = \left(1+\frac{m_\mathrm{t}^2}{\omega^2}\right)^{\sigma/2}.\end{aligned} \tag{4.7}$$

The frequency dependence of $\alpha_\mathrm{q}(\omega)$ is weak at high energy $\omega \gg m_\mathrm{t}$, but it shows in the soft γ-ray band relevant for GRB spectra. In the low-frequency regime, we find $\alpha_\mathrm{q}(\omega\to 0) \propto \omega^{-2\sigma}$, and the constant $\alpha_\mathrm{t} = q_\mathrm{t}^2/(4\pi\hbar c)$ is recovered at high frequencies, $\alpha_\mathrm{q}(\infty) = \alpha_\mathrm{t}$. The nonlocal charge and current densities depending on the varying coupling constant $q(\omega) = q_\mathrm{t}\hat{\Omega}(\omega)$ are denoted by a subscript Ω,

$$\begin{aligned}\hat{\rho}_\Omega(\mathbf{x},\omega) &= \hat{\Omega}(\omega)\hat{\rho}(\mathbf{x},\omega),\\ \hat{\mathbf{j}}_\Omega(\mathbf{x},\omega) &= \hat{\Omega}(\omega)\hat{\mathbf{j}}(\mathbf{x},\omega),\end{aligned} \tag{4.8}$$

with $(\hat{\rho},\hat{\mathbf{j}})$ as in (4.4) and $\hat{\Omega}(\omega)$ in (4.7). In the field equations (4.1), we replace $(\hat{\rho},\hat{\mathbf{j}})$ by $(\hat{\rho}_\Omega,\hat{\mathbf{j}}_\Omega)$. Occasionally, we will rescale $\hat{\omega} := \omega/m_\mathrm{t}$, so that $\upsilon_\mathrm{t} = \sqrt{1+\hat{\omega}^2}/\hat{\omega}$, and $\alpha_\mathrm{q} = \alpha_\mathrm{t}(1+\hat{\omega}^2)^\sigma/\hat{\omega}^{2\sigma}$. To find the tachyon potential generated by the current $(\hat{\rho}_\Omega,\hat{\mathbf{j}}_\Omega)$, we only need to multiply the local charge and current densities with $\hat{\Omega}(\omega)$, which amounts to a rescaling of the Fourier amplitudes $(\hat{A}_0,\hat{\mathbf{A}})$ in (4.3) by the same factor.

In real time, relations (4.8) among the Fourier amplitudes translate into

$$\begin{aligned}\rho_\Omega(\mathbf{x},t) &= \frac{1}{2\pi}\int_{-\infty}^{\infty}\hat{\rho}_\Omega(\mathbf{x},\omega)\mathrm{e}^{-\mathrm{i}\omega t}\,\mathrm{d}\omega\\ &= \int_{-\infty}^{\infty}\Omega(t')\rho(\mathbf{x},t-t')\,\mathrm{d}t',\\ \mathbf{j}_\Omega(\mathbf{x},t) &= \frac{1}{2\pi}\int_{-\infty}^{\infty}\hat{\mathbf{j}}_\Omega(\mathbf{x},\omega)\mathrm{e}^{-\mathrm{i}\omega t}\,\mathrm{d}\omega\\ &= \int_{-\infty}^{\infty}\Omega(t')\mathbf{j}(\mathbf{x},t-t')\,\mathrm{d}t',\end{aligned} \tag{4.9}$$

where

$$\Omega(t) = \frac{1}{2\pi}\int_{-\infty}^{\infty}\hat{\Omega}(\omega)\mathrm{e}^{-\mathrm{i}\omega t}\,\mathrm{d}\omega = \delta(t) + \Omega_\mathrm{reg}(t) \tag{4.10}$$

is a distribution with regular part

$$\begin{aligned}\Omega_\mathrm{reg}(t) &= \frac{1}{2\pi}\int_{-\infty}^{\infty}\hat{\Omega}_\mathrm{reg}(\omega)\mathrm{e}^{-\mathrm{i}\omega t}\,\mathrm{d}\omega,\\ \hat{\Omega}_\mathrm{reg}(\omega) &= \hat{\Omega}(\omega) - 1.\end{aligned} \tag{4.11}$$

The integral in (4.11) converges for exponents $\sigma < 1$, cf. (4.7), which is henceforth assumed; the time asymptotics of $\Omega_\mathrm{reg}(t)$ is studied in Appendix A.

The convolutions in (4.8) and (4.9) are modeled like the tachyonic inductions (2.2), but applied to the current and charge densities rather than to the field strengths, the counterpart of the permittivity $\varepsilon(t)$ being $\Omega(t)$. The analog to $\hat{\mathbf{j}}_\Omega(\mathbf{x},\omega)$ in (4.9) is the electric induction $\hat{\mathbf{D}}(\mathbf{x},\omega) = \hat{\varepsilon}(\omega)\hat{\mathbf{E}}(\mathbf{x},\omega)$, which reads in real space

$$\mathbf{D}(\mathbf{x},t) = \mathbf{E}(\mathbf{x},t) + \int_{-\infty}^{+\infty}\kappa(t')\mathbf{E}(\mathbf{x},t-t')\,\mathrm{d}t', \tag{4.12}$$

where $\varepsilon(t) = \delta(t) + \kappa(t)$ [28]. This is to be compared to (4.9) and (4.10). $\kappa(t)$ denotes the electric susceptibility, whose Fourier transform,

$$\hat{\kappa}(\omega) = \hat{\varepsilon}(\omega) - 1, \quad \hat{\varepsilon}(\omega) = \int_{-\infty}^{+\infty}\varepsilon(t)\mathrm{e}^{\mathrm{i}\omega t}\,\mathrm{d}t, \tag{4.13}$$

is the analog to $\hat{\Omega}_\mathrm{reg}(\omega)$ in (4.11). The counterpart to the electric polarization $\hat{\mathbf{D}} - \hat{\mathbf{E}} = \hat{\kappa}\hat{\mathbf{E}}$ is the charge and current dispersion, $\hat{\rho}_\Omega - \hat{\rho} = \hat{\Omega}_\mathrm{reg}\hat{\rho}$ and $\hat{\mathbf{j}}_\Omega - \hat{\mathbf{j}} = \hat{\Omega}_\mathrm{reg}\hat{\mathbf{j}}$, generated by the frequency-dependent coupling constant.

We consider a subluminal charge in uniform motion, $z = \upsilon t$. The charge density and current along the z axis and the respective Fourier amplitudes read, cf. after (4.3),

$$\rho(\mathbf{x},t) = q_\mathrm{t}\delta(x)\delta(y)\delta(z-\upsilon t), \qquad j(\mathbf{x},t) = \upsilon\rho(\mathbf{x},t),$$
$$\hat\rho(\mathbf{x},\omega) = \frac{q_\mathrm{t}}{|\upsilon|}\delta(x)\delta(y)\mathrm{e}^{\mathrm{i}\omega z/\upsilon}, \qquad \hat j = \upsilon\hat\rho. \tag{4.14}$$

Replacing q_t by $q(\omega) = q_\mathrm{t}\hat\Omega(\omega)$, we arrive at the nonlocal current $(\hat\rho_\Omega, \hat{\mathbf{j}}_\Omega)$ as defined in (4.8). In real time, cf. (4.9),

$$\rho_\Omega(\mathbf{x},t) = \frac{q_\mathrm{t}}{|\upsilon|}\Omega(t-z/\upsilon)\delta(x)\delta(y),$$
$$j_\Omega(\mathbf{x},t) = \upsilon\rho_\Omega(\mathbf{x},t). \tag{4.15}$$

The x and y components of $\mathbf{j}_\Omega$ vanish. We split Ω into a regular and singular part, cf. (4.10),

$$\rho_\Omega(\mathbf{x},t) = q_\mathrm{t}\left[\delta(z-\upsilon t) + \frac{1}{|\upsilon|}\Omega_\mathrm{reg}(t-z/\upsilon)\right]\delta(x)\delta(y). \tag{4.16}$$

For negative scaling exponents σ, the total charge $\int \rho_\Omega(\mathbf{x},t)\,\mathrm{d}^3x$ vanishes, since

$$\int_{-\infty}^{\infty}\Omega_\mathrm{reg}(t-z/\upsilon)\,\mathrm{d}z = |\upsilon|\hat\Omega_\mathrm{reg}(0), \tag{4.17}$$

and $\hat\Omega_\mathrm{reg}(0) = -1$, cf. (4.7) and (4.11). If $0 < \sigma < 1$, then $\hat\Omega_\mathrm{reg}(0)$ is infinite, and so is the total charge. The space and time evolution of the nonlocal regular part of charge density (4.16) is determined by $\Omega_\mathrm{reg}(t-z/\upsilon)$, cf. Appendix A.

5 Tachyonic conductivity of an electron plasma

We start with a monochromatic superluminal mode, $\mathbf{E}(\mathbf{x},t) = \hat{\mathbf{E}}(\mathbf{x},\omega)\mathrm{e}^{-\mathrm{i}\omega t} + \mathrm{c.c.}$, in a dispersive and dissipative medium, generating the current

$$\hat{\mathbf{j}} = \sigma(\omega)\hat{\mathbf{E}}, \qquad \hat\rho = \frac{\sigma}{\mathrm{i}\omega}\operatorname{div}\hat{\mathbf{E}}, \tag{5.1}$$

where $\sigma(\omega)$ is the tachyonic conductivity specified in (5.5). The hat always indicates Fourier amplitudes, and the charge distribution $\hat\rho$ is found by current conservation, cf. after (2.5). We substitute this into the field equations (2.1), and absorb the current and charge densities by replacing the permittivity ε by

$$\varepsilon_\sigma(\omega) := \left(1 + \mathrm{i}\frac{\sigma(\omega)}{\varepsilon\omega}\right)\varepsilon. \tag{5.2}$$

In this way, we can write the inhomogeneous field equations (2.4) as

$$\operatorname{rot}\hat{\mathbf{B}} + \mathrm{i}\varepsilon_\sigma\mu\omega\hat{\mathbf{E}} = m_\mathrm{t}^2\frac{\mu}{\mu_0}\hat{\mathbf{A}}, \qquad \operatorname{div}\hat{\mathbf{E}} = -m_\mathrm{t}^2\frac{\varepsilon_0}{\varepsilon_\sigma}\hat A_0. \tag{5.3}$$

The homogeneous Maxwell equations in (2.1) remain unchanged. If $\varepsilon = 1$ in (5.2), we find the polarization $\hat{\mathbf{P}} = \hat{\mathbf{D}} - \hat{\mathbf{E}} = \mathrm{i}(\sigma/\omega)\hat{\mathbf{E}}$. The dispersion relations for the transversal and longitudinal modes read as in (3.4) and (3.8), with ε replaced by ε_σ. Current and charge densities are related to the tachyonic field strength $\hat{\mathbf{E}}$ by (5.1), so that the potentials $(\hat A_0, \hat{\mathbf{A}})$ are unambiguously determined by the charge density and current,

$$\hat A_0 = \frac{\omega}{\mathrm{i}\sigma m_\mathrm{t}^2}\frac{\varepsilon_\sigma}{\varepsilon_0}\hat\rho, \qquad \hat{\mathbf{A}} = \frac{1}{\mathrm{i}\sigma\omega}\hat{\mathbf{j}} + \frac{1}{\sigma m_\mathrm{t}^2}\frac{\varepsilon_\sigma}{\varepsilon_0}\nabla\hat\rho. \tag{5.4}$$

Taking the rotor of the second equation in (5.4), we find the London equation $\operatorname{rot}\hat{\mathbf{j}} = \mathrm{i}\sigma\omega\hat{\mathbf{B}}$. On substituting this into wave equation (2.6) for the magnetic field strength, we arrive at $(\Delta + k_\mathrm{T}^2)\hat{\mathbf{B}} = 0$, where the squared transversal wave number is defined in (3.4) (with $\varepsilon \to \varepsilon_\sigma$).

The tachyonic conductivity reads

$$\sigma(\omega) = \frac{\mathrm{i}\omega_\mathrm{p}^2\omega}{\omega^2 - \omega_0^2 + \mathrm{i}\gamma_0\omega}, \qquad \omega_\mathrm{p}^2 := q^2(\omega)\frac{n_\mathrm{e}}{m}, \tag{5.5}$$

where ω_p is the tachyonic plasma frequency, m the electron mass, n_e the electron density of the medium, and $q(\omega) = q_\mathrm{t}\hat\Omega(\omega)$ the frequency-dependent tachyonic coupling constant, cf. (4.5)–(4.7). This is based on Drude's damped oscillator model with a nonlocal coupling to the field strength [2],

$$\ddot{\mathbf{r}} + \gamma_0\dot{\mathbf{r}} + \omega_0^2\mathbf{r} = \frac{1}{m}\int_{-\infty}^{+\infty} q(t')\mathbf{E}(t-t')\,\mathrm{d}t', \tag{5.6}$$

with $\mathbf{r} = \hat{\mathbf{r}}\mathrm{e}^{-\mathrm{i}\omega t} + \mathrm{c.c.}$, $\mathbf{E}$ as defined before (5.1), and $q(t) := q_\mathrm{t}\Omega(t)$, cf. (4.10). ω_0 is the characteristic frequency of the electronic oscillators, and γ_0 the damping constant, related to the resistivity ρ and relaxation time τ as $\gamma_0 = \omega_\mathrm{p}^2\rho = 1/\tau$. When solving this equation in dipole approximation (with a plane wave $\mathbf{E}$ as in Sect. 3), we neglect the spatial dependence of the amplitude $\hat{\mathbf{E}}(\mathbf{x},\omega)$, so that $(\omega_0^2 - \omega^2 - \mathrm{i}\gamma_0\omega)\hat{\mathbf{r}} = q(\omega)\hat{\mathbf{E}}/m$, and $\sigma(\omega)$ in (5.5) follows from $\hat{\mathbf{j}} = q(\omega)n_\mathrm{e}\hat{\mathbf{v}}$, with $\hat{\mathbf{v}} = -\mathrm{i}\omega\hat{\mathbf{r}}$. We note $\omega_\mathrm{p}^2 = \omega_{\mathrm{p,em}}^2\alpha_\mathrm{q}/\alpha_\mathrm{e}$, where $\omega_\mathrm{p,em}$ is the electromagnetic plasma frequency, $\alpha_\mathrm{e} = e^2/(4\pi\hbar c) \approx 1/137$ the electric fine-structure constant, and $\alpha_\mathrm{q}(\omega) = \alpha_\mathrm{t}\hat\Omega^2(\omega)$ its frequency-dependent tachyonic counterpart, cf. (4.7). Thus, $\omega_\mathrm{p}^2 = \hat\Omega^2(\omega)\omega_\mathrm{p,em}^2\alpha_\mathrm{t}/\alpha_\mathrm{e}$; the typical range of the tachyon mass m_t for γ-ray bursts is 10^2–10^4 keV, with α_t in the range 10^{-21}–10^{-23}, cf. Ref. [3] and Sect. 6.

The damping constant γ_0 is related to the resistivity by $\hbar\gamma_0[\mathrm{eV}] \approx 1.690\times10^3(\hbar\omega_\mathrm{p}[\mathrm{eV}])^2\rho[\Omega\,\mathrm{cm}]$(with conversion $\Omega \approx 1.113\times10^{-12}$ s/cm) and to the relaxation time by $\tau[\mathrm{s}] \approx 6.582\times10^{-16}/(\hbar\gamma_0[\mathrm{eV}])$. In the following, we assume the permeabilities $(\varepsilon_0, \varepsilon)$ and (μ_0, μ) in (5.2)–(5.4) to be positive and frequency independent; in the dispersion relations, ε is replaced by ε_σ, cf. (5.2) and (5.5), and the same

substitution is performed in the plane-wave solutions (3.6) and (3.9) as well as in the flux vectors (3.19).

5.1 Transversal dispersion relation and relaxation time asymptotics

The transversal dispersion relation (3.4) reads $k_\mathrm{T}^2 = \varepsilon_\sigma \mu\omega^2 + m_\mathrm{t}^2 \mu/\mu_0$, with ε_σ defined in (5.2) and (5.5). As for the root, positivity of the real part of $k_\mathrm{T}(\omega)$ is necessary to obtain waves propagating in the direction of $\mathbf{k}_0$, and a positive imaginary part is required for exponential damping. We put $\gamma_0 = 1/\tau_\mathrm{T}$ in (5.5), where τ_T is the transversal relaxation time (related to the transversal resistivity by $\tau_\mathrm{T}\omega_\mathrm{p}^2 = 1/\rho_\mathrm{T}$), and rescale the tachyonic plasma frequency for notational convenience, $\omega_{\mathrm{p},\varepsilon}^2 := \omega_\mathrm{p}^2/\varepsilon$. In the limit $\tau_\mathrm{T} \to 0$, the squared wave number reads

$$k_\mathrm{T}^2 \sim k_{\mathrm{T},0}^2 + \mathrm{i}\varepsilon\mu\omega_{\mathrm{p},\varepsilon}^2\omega\tau_\mathrm{T}, \qquad k_{\mathrm{T},0}^2 := \varepsilon\mu\omega^2 + m_\mathrm{t}^2\frac{\mu}{\mu_0}, \tag{5.7}$$

where only the leading orders of the real and imaginary parts are indicated. The permeabilities $(\varepsilon_0, \varepsilon)$ and (μ_0, μ) are positive frequency-independent constants. In the opposite limit, $\tau_\mathrm{T} \to \infty$,

$$k_\mathrm{T}^2 \sim k_{\mathrm{T},0}^2 - \frac{\varepsilon\mu\omega_{\mathrm{p},\varepsilon}^2\omega^2}{\omega^2-\omega_0^2} + \mathrm{i}\frac{\varepsilon\mu\omega_{\mathrm{p},\varepsilon}^2\omega^3}{(\omega^2-\omega_0^2)^2}\frac{1}{\tau_\mathrm{T}}. \tag{5.8}$$

The exact transversal dispersion relation is

$$k_\mathrm{T}^2 = k_{\mathrm{T},0}^2 + \mathrm{i}\sigma\mu\omega = k_{\mathrm{T},0}^2 - \frac{\varepsilon\mu\omega_{\mathrm{p},\varepsilon}^2\omega^2}{\omega^2-\omega_0^2+\mathrm{i}\gamma_0\omega}, \tag{5.9}$$

with $\gamma_0 = 1/\tau_\mathrm{T}$ and $k_{\mathrm{T},0}^2$ as defined in (5.7). The root k_T of (5.9) is chosen with positive real and imaginary part, which is possible for positive τ_T. The transversal wave number in the high-resistivity regime, $\tau_\mathrm{T} \to 0$, reads, cf. (5.7),

$$\mathrm{Re}(k_\mathrm{T}) \sim k_{\mathrm{T},0}, \qquad \mathrm{Im}(k_\mathrm{T}) \sim \frac{\tau_\mathrm{T}}{2}\varepsilon\mu\omega_{\mathrm{p},\varepsilon}^2\frac{\omega}{k_{\mathrm{T},0}}, \tag{5.10}$$

with $k_{\mathrm{T},0} > 0$, cf. (5.7). At low resistivity, $\tau_\mathrm{T} \to \infty$, there is a dichotomy depending on the sign of

$$K_{\mathrm{T},\infty}(\omega) := k_{\mathrm{T},0}^2 - \varepsilon\mu\frac{\omega_{\mathrm{p},\varepsilon}^2\omega^2}{\omega^2-\omega_0^2}. \tag{5.11}$$

If $K_{\mathrm{T},\infty}$ is positive, the asymptotic ($\tau_\mathrm{T} \to \infty$) wave number is found as

$$\begin{aligned}\mathrm{Re}(k_\mathrm{T}) &\sim \sqrt{K_{\mathrm{T},\infty}},\\ \mathrm{Im}(k_\mathrm{T}) &\sim \frac{1}{2\tau_\mathrm{T}}\frac{\varepsilon\mu\omega_{\mathrm{p},\varepsilon}^2\omega^3}{\sqrt{K_{\mathrm{T},\infty}}(\omega^2-\omega_0^2)^2},\end{aligned} \tag{5.12}$$

and if $K_{\mathrm{T},\infty}$ is negative, the real and imaginary parts are interchanged,

$$\begin{aligned}\mathrm{Re}(k_\mathrm{T}) &\sim \frac{1}{2\tau_\mathrm{T}}\frac{\varepsilon\mu\omega_{\mathrm{p},\varepsilon}^2\omega^3}{\sqrt{|K_{\mathrm{T},\infty}|}(\omega^2-\omega_0^2)^2},\\ \mathrm{Im}(k_\mathrm{T}) &\sim \sqrt{|K_{\mathrm{T},\infty}|}.\end{aligned} \tag{5.13}$$

Sign changes of $K_{\mathrm{T},\infty}(\omega)$ (which is just the squared wave number k_T^2 at $\gamma_0 = 0$) can thus substantially affect tachyonic wave propagation at low resistivity, cf. Sect. 5.3. The transversal flux vector $\langle \mathbf{S}^\mathrm{T} \rangle$ is obtained by substituting $2\,\mathrm{Re}(k_\mathrm{T})/\mu$ for the ratio in (3.19). The transversal wavelength $\lambda_\mathrm{T} = 2\pi/\mathrm{Re}(k_\mathrm{T})$ and the tachyonic attenuation length $\delta_\mathrm{T} = 1/\mathrm{Im}(k_\mathrm{T})$ in the high/low-resistivity regime can also be read off from these limits. The wave fields as well as the current and charge densities are damped by a factor of $\exp(-\mathbf{k}_0\mathbf{x}/\delta_\mathrm{T})$ in the direction of propagation $\mathbf{k}_0$. The electromagnetic dispersion relation is recovered by replacing $\omega_{\mathrm{p},\varepsilon}^2$ by the rescaled electromagnetic plasma frequency $\omega_{\mathrm{p,em}}^2/\varepsilon$ and dropping the tachyon mass in (5.7) and (5.9). We then have to replace $K_{\mathrm{T},\infty}$ in (5.11) by

$$K_{\mathrm{em},\infty} := \frac{\varepsilon\mu\omega^2}{\omega^2-\omega_0^2}\left(\omega^2 - \omega_0^2 - \frac{1}{\varepsilon}\omega_{\mathrm{p,em}}^2\right). \tag{5.14}$$

If $K_{\mathrm{em},\infty}$ is negative, we find the electromagnetic attenuation length at low resistivity as $\delta_\mathrm{em} \sim 1/\sqrt{|K_{\mathrm{em},\infty}|}$, cf. (5.13).

5.2 Longitudinal conductivity and extinction coefficient

The conductivity (5.5) requires a negative longitudinal damping constant, $\gamma_0 = -1/\tau_\mathrm{L}$, for the wave number k_L to admit positive real and imaginary parts. The magnetic permeability μ does not show in the dispersion relation, $k_\mathrm{L}^2 = \varepsilon_0\mu_0\omega^2 + m_\mathrm{t}^2\varepsilon_0/\varepsilon_\sigma$, cf. (3.8), as there is no longitudinal magnetic wave component. In the limit $\tau_\mathrm{L} \to 0$, we find

$$\begin{aligned}k_\mathrm{L}^2 &\sim k_{\mathrm{L},0}^2 + \mathrm{i}\frac{\varepsilon_0}{\varepsilon}\frac{\omega_{\mathrm{p},\varepsilon}^2}{\omega}m_\mathrm{t}^2\tau_\mathrm{L},\\ k_{\mathrm{L},0}^2 &:= \varepsilon_0\mu_0\omega^2 + m_\mathrm{t}^2\frac{\varepsilon_0}{\varepsilon},\end{aligned} \tag{5.15}$$

and in the opposite limit, $\tau_\mathrm{L} \to \infty$,

$$\begin{aligned}k_\mathrm{L}^2 \sim k_{\mathrm{L},0}^2 &+ \frac{\varepsilon_0}{\varepsilon}\frac{m_\mathrm{t}^2\omega_{\mathrm{p},\varepsilon}^2}{\omega^2-\omega_0^2-\omega_{\mathrm{p},\varepsilon}^2}\\ &+ \mathrm{i}\frac{\varepsilon_0}{\varepsilon}\frac{m_\mathrm{t}^2\omega_{\mathrm{p},\varepsilon}^2\omega}{(\omega^2-\omega_0^2-\omega_{\mathrm{p},\varepsilon}^2)^2}\frac{1}{\tau_\mathrm{L}}.\end{aligned} \tag{5.16}$$

The exact longitudinal dispersion relation reads

$$\begin{aligned}k_\mathrm{L}^2 &= k_{\mathrm{L},0}^2 - \frac{\varepsilon_0}{\varepsilon}\frac{\mathrm{i}\sigma m_\mathrm{t}^2}{\varepsilon\omega+\mathrm{i}\sigma}\\ &= k_{\mathrm{L},0}^2 + \frac{\varepsilon_0}{\varepsilon}\frac{m_\mathrm{t}^2\omega_{\mathrm{p},\varepsilon}^2}{\omega^2-\omega_0^2-\omega_{\mathrm{p},\varepsilon}^2+\mathrm{i}\gamma_0\omega},\end{aligned} \tag{5.17}$$

with $\gamma_0 = -1/\tau_\mathrm{L}$ and $k_{\mathrm{L},0}^2$ in (5.15); the permeabilities $(\varepsilon_0, \varepsilon)$ and μ_0 are positive constants. Relaxation time and longitudinal resistivity are related by $\tau_\mathrm{L} = 1/(\rho_\mathrm{L}\omega_\mathrm{p}^2)$. Returning to (5.1), we find the polarized current components $\hat{\mathbf{j}}^{\mathrm{T,L}} = \sigma_{\mathrm{T,L}}\hat{\mathbf{E}}^{\mathrm{T,L}}$, where $\sigma_\mathrm{T} = \sigma(\omega; \gamma_0 = 1/\tau_\mathrm{T})$ and $\sigma_\mathrm{L} = \sigma(\omega; \gamma_0 = -1/\tau_\mathrm{L})$ are the respective transversal and longitudinal conductivities (5.5), and $\hat{\mathbf{E}}^{\mathrm{T,L}}$ the polarized field strengths, cf. (3.5) and (3.9). We may put $\sigma_\mathrm{T} = \sum \sigma_{\mathrm{T},i}$, where the conductivities $\sigma_{\mathrm{T},i}$ are defined as in (5.5), with constants $(\omega_{\mathrm{p},i}^2, \omega_{0,i}, \gamma_{0,i} = 1/\tau_{\mathrm{T},i})$ characterizing the oscillator species [25], and analogously for σ_L.

The longitudinal tachyonic extinction coefficient, $\delta_\mathrm{L} = 1/\mathrm{Im}(k_\mathrm{L})$, is obtained via (5.15) and (5.16) or from (5.17) in case of moderate relaxation time or in the vicinity of the resonances. For short relaxation times, $\tau_\mathrm{L} \to 0$, we find the longitudinal wave number

$$\mathrm{Re}(k_\mathrm{L}) \sim k_{\mathrm{L},0}, \qquad \mathrm{Im}(k_\mathrm{L}) \sim \frac{\tau_\mathrm{L}}{2}\frac{\varepsilon_0}{\varepsilon}\frac{m_\mathrm{t}^2\omega_{\mathrm{p},\varepsilon}^2}{k_{\mathrm{L},0}\omega}, \tag{5.18}$$

with positive $k_{\mathrm{L},0}$, cf. (5.15). As for the opposite limit, the low-resistivity regime $\tau_\mathrm{L} \to \infty$, we define the shortcut

$$K_{\mathrm{L},\infty}(\omega) := k_{\mathrm{L},0}^2 + \frac{\varepsilon_0}{\varepsilon}\frac{m_\mathrm{t}^2\omega_{\mathrm{p},\varepsilon}^2}{\omega^2 - \omega_0^2 - \omega_{\mathrm{p},\varepsilon}^2}, \tag{5.19}$$

which coincides with k_L^2 at $\gamma_0 = 0$, cf. (5.16). The longitudinal asymptotic ($\tau_\mathrm{L} \to \infty$) wave number reads, for $K_{\mathrm{L},\infty} > 0$,

$$\begin{aligned}\mathrm{Re}(k_\mathrm{L}) &\sim \sqrt{K_{\mathrm{L},\infty}},\\ \mathrm{Im}(k_\mathrm{L}) &\sim \frac{1}{2\tau_\mathrm{L}}\frac{\varepsilon_0}{\varepsilon}\frac{m_\mathrm{t}^2\omega_{\mathrm{p},\varepsilon}^2\omega}{\sqrt{K_{\mathrm{L},\infty}}(\omega^2 - \omega_0^2 - \omega_{\mathrm{p},\varepsilon}^2)^2},\end{aligned} \tag{5.20}$$

and for $K_{\mathrm{L},\infty} < 0$,

$$\begin{aligned}\mathrm{Re}(k_\mathrm{L}) &\sim \frac{1}{2\tau_\mathrm{L}}\frac{\varepsilon_0}{\varepsilon}\frac{m_\mathrm{t}^2\omega_{\mathrm{p},\varepsilon}^2\omega}{\sqrt{|K_{\mathrm{L},\infty}|}(\omega^2 - \omega_0^2 - \omega_{\mathrm{p},\varepsilon}^2)^2},\\ \mathrm{Im}(k_\mathrm{L}) &\sim \sqrt{|K_{\mathrm{L},\infty}|}.\end{aligned} \tag{5.21}$$

The longitudinal tachyonic flux vector $\langle \mathbf{S}^\mathrm{L}\rangle$ in the high/low-resistivity regime is found by replacing the first ratio in (3.19) by $2\,\mathrm{Re}(k_\mathrm{L})/(\mu_0^2\varepsilon_0)$, with the respective asymptotic $\mathrm{Re}(k_\mathrm{L})$ substituted. The transversal and longitudinal wavelengths $\lambda_{\mathrm{T,L}} = 2\pi/\mathrm{Re}(k_{\mathrm{T,L}})$ can become arbitrarily large in the low-resistivity regime, cf. Sect. 5.3. By contrast, the tachyonic wavelength in vacuum cannot exceed the Compton wavelength $\lambda_\mathrm{t} = 2\pi/m_\mathrm{t}$, since the vacuum dispersion relation is $k^2 = \omega^2 + m_\mathrm{t}^2$, irrespectively of the polarization. The longitudinal extinction coefficient, $\delta_\mathrm{L} = 1/\mathrm{Im}(k_\mathrm{L})$, is obtained from the $\mathrm{Im}(k_\mathrm{L})$ limits enumerated in (5.18)–(5.21), or calculated from the exact dispersion relation (5.17).

5.3 The limit of zero resistivity

The tachyonic conductivity (5.5) reduces to $\sigma(\omega) = \mathrm{i}\omega_\mathrm{p}^2/\omega$, for transversal and longitudinal modes alike, if we consider the limit of infinite relaxation time, $\tau_{\mathrm{T,L}} = \infty$, in the absence of harmonic binding, $\omega_0 = 0$, and use vacuum permeabilities, $\varepsilon = \varepsilon_0 = 1$ and $\mu = \mu_0 = 1$. The induced permittivity (5.2) is thus $\varepsilon_\sigma = 1 - \omega_\mathrm{p}^2/\omega^2$, and the squared transversal wave numbers read $k_\mathrm{T}^2 = K_{\mathrm{T},\infty} = \omega^2 - \omega_\mathrm{p}^2 + m_\mathrm{t}^2$ and $K_{\mathrm{em},\infty} = \omega^2 - \omega_{\mathrm{p,em}}^2$, cf. (5.11) and (5.14). In the static limit $\omega = 0$, the electromagnetic attenuation length is $\delta_\mathrm{em} = 1/\omega_{\mathrm{p,em}}$, cf. after (5.14). Restoring the units $\hbar = c = 1$, we obtain $\hbar\omega_{\mathrm{p,em}}[\mathrm{eV}] \approx 1.973 \times 10^3/\delta_\mathrm{em}[\text{Å}]$. In superconductors, the electromagnetic penetration depth δ_em is typically of order 10^3 Å. We may write the electromagnetic plasma frequency as $\omega_{\mathrm{p,em}}^2 = 4\pi c^2 \lambda\!\!\!^{-}_\mathrm{e}\alpha_\mathrm{e} n_\mathrm{e}$, where $\lambda\!\!\!^{-}_\mathrm{e}$ is the reduced electronic Compton wavelength, α_e the electric fine-structure constant, and n_e the electron density. Hence, $\hbar\omega_{\mathrm{p,em}}[\mathrm{eV}] \approx 3.713 \times 10^{-11} n_\mathrm{e}^{1/2}[\mathrm{cm}^{-3}]$; electron densities of 10^{26} cm^{-3} can be reached in inertially or magnetically confined fusion plasmas [30, 31].

The tachyonic plasma frequency reads $\omega_\mathrm{p}^2 = \kappa^2\hat{\Omega}^2(\omega)$, where $\kappa^2 := \omega_{\mathrm{p,em}}^2\alpha_\mathrm{t}/\alpha_\mathrm{e}$, cf. after (5.6). For $\omega^2/m_\mathrm{t}^2 \ll 1$, we find, cf. (4.7),

$$\begin{aligned}\hat{\Omega}^2(\omega) &= \left(1 + \frac{m_\mathrm{t}^2}{\omega^2}\right)^\sigma\\ &= \left(\frac{m_\mathrm{t}^2}{\omega^2}\right)^\sigma\left(1 + \sigma\frac{\omega^2}{m_\mathrm{t}^2} + \cdots\right),\end{aligned} \tag{5.22}$$

with $0 < \sigma < 1$; typically $\sigma \approx 0.5$ for burst plasmas. Given the values of $\omega_{\mathrm{p,em}}$ quoted above (1–100 eV) and the relevant ranges of the tachyon mass $m_\mathrm{t} \approx 10^2$–$10^4$ keV and the tachyonic fine-structure constant $\alpha_\mathrm{t} \approx 10^{-21}$–$10^{-23}$, we can safely assume $\kappa/m_\mathrm{t} \ll 1$. As mentioned, the squared wave number k_T^2 is $K_{\mathrm{T},\infty}(\omega) = \omega^2 + m_\mathrm{t}^2 - \kappa^2\hat{\Omega}^2(\omega)$, admitting a zero $K_{\mathrm{T},\infty}(\omega_\mathrm{T}) = 0$ at

$$\frac{\omega_\mathrm{T}}{m_\mathrm{t}} = \left(\frac{\kappa}{m_\mathrm{t}}\right)^{1/\sigma}\left(1 + \frac{\sigma - 1}{2\sigma}\left(\frac{\kappa}{m_\mathrm{t}}\right)^{2/\sigma} + \cdots\right). \tag{5.23}$$

Apparently, $\omega_\mathrm{T} \ll m_\mathrm{t}$, and $K_{\mathrm{T},\infty}(\omega)$ is positive for $\omega > \omega_\mathrm{T}$ and negative otherwise. If $K_{\mathrm{T},\infty}$ is positive, there is no attenuation of transversally propagating modes in the limit of infinite relaxation time. In this case, the transversal tachyonic flux vector and energy density are obtained from (3.21) and (3.24) (with $\varepsilon \to \varepsilon_\sigma$ and $\mu = \mu_0 = \varepsilon_0 = 1$),

$$\langle \mathbf{S}^\mathrm{T}\rangle = 2\omega\sqrt{K_{\mathrm{T},\infty}}\,|\hat{\mathbf{A}}^\mathrm{T}|^2\mathbf{k}_0, \qquad \langle \rho^\mathrm{T}\rangle = \omega\frac{\mathrm{d}k_\mathrm{T}^2}{\mathrm{d}\omega}|\hat{\mathbf{A}}^\mathrm{T}|^2, \tag{5.24}$$

where

$$K_{\mathrm{T},\infty} = k_{\mathrm{T}}^2 = \omega^2 - \omega_{\mathrm{p}}^2 + m_{\mathrm{t}}^2,$$
$$\frac{\mathrm{d}k_{\mathrm{T}}^2}{\mathrm{d}\omega} = 2\omega\left(1 + \frac{\sigma}{1+\omega^2/m_{\mathrm{t}}^2}\frac{\omega_{\mathrm{p}}^2}{\omega^2}\right). \tag{5.25}$$

This is valid for $\omega > \omega_{\mathrm{T}}$, cf. (5.23), where $K_{\mathrm{T},\infty}$ is positive. The energy density (5.24) can also be recovered from (3.25), with

$$\frac{\mathrm{d}\hat{\Omega}^2}{\mathrm{d}\omega} = -\frac{2\sigma}{\omega}\frac{\hat{\Omega}^2}{1+\omega^2/m_{\mathrm{t}}^2},$$
$$\varepsilon'_\sigma(\omega) = 2\frac{\omega_{\mathrm{p}}^2}{\omega^3}\left(1 + \frac{\sigma}{1+\omega^2/m_{\mathrm{t}}^2}\right). \tag{5.26}$$

The transversal group velocity is obtained from (5.25), $\upsilon_{\mathrm{T}} = 2\sqrt{K_{\mathrm{T},\infty}}\,\mathrm{d}\omega/\mathrm{d}k_{\mathrm{T}}^2$.

Next we consider frequencies $\omega < \omega_{\mathrm{T}}$, where $K_{\mathrm{T},\infty}(\omega)$ is negative. The transversal attenuation length reads $\delta_{\mathrm{T}} = 1/\sqrt{|K_{\mathrm{T},\infty}|}$, cf. after (5.13), with $K_{\mathrm{T},\infty}$ in (5.25). As the transversal tachyon flux $\langle \mathbf{S}^{\mathrm{T}}\rangle \propto \mathrm{Re}(k_{\mathrm{T}})$ vanishes in the limit $\tau_{\mathrm{T}} \to \infty$, cf. (5.13), transversal frequencies below $\omega < \omega_{\mathrm{T}}$ are totally reflected.

We turn to the longitudinal dispersion relation at zero resistivity ($\gamma_0 = 0$), which reads $k_{\mathrm{L}}^2 =: K_{\mathrm{L},\infty} = K_{\mathrm{T},\infty}\omega^2/(\omega^2 - \omega_{\mathrm{p}}^2)$, cf. (5.19). The zero ω_{L} of the denominator $\omega^2 - \omega_{\mathrm{p}}^2$ is found as

$$\frac{\omega_{\mathrm{L}}}{m_{\mathrm{t}}} = \left(\frac{\kappa}{m_{\mathrm{t}}}\right)^{1/(\sigma+1)} \times \left(1 + \frac{\sigma}{2(\sigma+1)}\left(\frac{\kappa}{m_{\mathrm{t}}}\right)^{2/(\sigma+1)} + \cdots\right), \tag{5.27}$$

where we use $\kappa/m_{\mathrm{t}} \ll 1$ as in (5.23). Clearly, $\omega_{\mathrm{L}} \ll m_{\mathrm{t}}$, and $\omega^2 - \omega_{\mathrm{p}}^2$ is positive for $\omega > \omega_{\mathrm{L}}$. Since the exponent σ is positive, we have $\omega_{\mathrm{T}} < \omega_{\mathrm{L}}$, where ω_{T} is the zero of $K_{\mathrm{T},\infty}(\omega)$, cf. (5.23). Thus $K_{\mathrm{L},\infty}$ is positive in the intervals $\omega < \omega_{\mathrm{T}}$ and $\omega > \omega_{\mathrm{L}}$, where the longitudinal flux and energy densities are obtained from (3.21), (3.24), and (3.25),

$$\langle \mathbf{S}^{\mathrm{L}}\rangle = 2\frac{m_{\mathrm{t}}^2}{\omega}\sqrt{K_{\mathrm{L},\infty}}\,|\hat{\mathbf{A}}^{\mathrm{L}}|^2\mathbf{k}_0,$$
$$\langle \rho^{\mathrm{L}}\rangle = \frac{m_{\mathrm{t}}^2}{\omega}\frac{\mathrm{d}k_{\mathrm{L}}^2}{\mathrm{d}\omega}|\hat{\mathbf{A}}^{\mathrm{L}}|^2, \tag{5.28}$$

by substitution of

$$K_{\mathrm{L},\infty} = k_{\mathrm{L}}^2 = \omega^2\left(1 + \frac{m_{\mathrm{t}}^2}{\omega^2 - \omega_{\mathrm{p}}^2}\right),$$
$$\frac{\mathrm{d}k_{\mathrm{L}}^2}{\mathrm{d}\omega} = 2\omega\left(1 - \frac{m_{\mathrm{t}}^2\omega_{\mathrm{p}}^2}{(\omega^2-\omega_{\mathrm{p}}^2)^2}\left(1 + \frac{\sigma}{1+\omega^2/m_{\mathrm{t}}^2}\right)\right). \tag{5.29}$$

The longitudinal group velocity reads $\upsilon_{\mathrm{L}} = 2\sqrt{K_{\mathrm{L},\infty}}\,\mathrm{d}\omega/\mathrm{d}k_{\mathrm{L}}^2$. In the vicinity of $\omega \approx \omega_{\mathrm{L}}$ (but still $\omega > \omega_{\mathrm{L}}$), υ_{L} is negative, since ω_{L} is the zero of $\omega^2 - \omega_{\mathrm{p}}^2$. In this case, we have to change the sign of $\langle \mathbf{S}^{\mathrm{L}}\rangle$ and $\langle \rho^{\mathrm{L}}\rangle$ in (5.28). As υ_{L} is negative and $\langle \mathbf{S}^{\mathrm{L}}\rangle = \mathbf{k}_0\upsilon_{\mathrm{L}}\langle \rho^{\mathrm{L}}\rangle$, the longitudinal energy transfer happens in the opposite direction of the wave vector [17, 18].

$K_{\mathrm{L},\infty}(\omega)$ is negative in the interval $\omega_{\mathrm{T}} < \omega < \omega_{\mathrm{L}}$, where the longitudinal attenuation length is $\delta_{\mathrm{L}} = 1/\sqrt{|K_{\mathrm{L},\infty}|}$, with $K_{\mathrm{L},\infty}$ in (5.29). The flux $\langle \mathbf{S}^{\mathrm{L}}\rangle \propto \mathrm{Re}(k_{\mathrm{L}})$ vanishes in the limit $\tau_{\mathrm{L}} \to \infty$, cf. (5.21), and longitudinal waves with frequencies in this interval are totally reflected like transversal modes below ω_{T}. Outside this interval, the plasma becomes transparent for longitudinal modes, and the flux and energy densities (5.28) apply.

6 Superluminal radiation densities: tachyonic spectral fits of the γ-ray bursts GRB 930506, GRB 950425, and GRB 910503

The quantized tachyonic radiation densities of a uniformly moving electron read [21]

$$p^{\mathrm{T,L}}(\omega,\gamma) = m_{\mathrm{t}}^2\frac{\alpha_{\mathrm{q}}(\omega)\omega}{\omega^2+m_{\mathrm{t}}^2}\left[\gamma^2 - \frac{m_{\mathrm{t}}}{m}\frac{\omega}{m_{\mathrm{t}}}\gamma - \frac{1}{4}\frac{m_{\mathrm{t}}^2}{m^2} - \left(1+\frac{\omega^2}{m_{\mathrm{t}}^2}\right)\Delta^{\mathrm{T,L}}\right]\frac{1}{\gamma\sqrt{\gamma^2-1}}, \tag{6.1}$$

where the superscripts T and L refer to the transversal/longitudinal polarization components of the superluminal radiation defined by $\Delta^{\mathrm{T}} = 1 - m_{\mathrm{t}}^2/(2m^2)$ and $\Delta^{\mathrm{L}} = 0$. m and γ denote the mass and Lorentz factor of the electron, m_{t} is the tachyon mass, and $\alpha_{\mathrm{q}}(\omega) = \alpha_{\mathrm{t}}\hat{\Omega}^2(\omega)$ the tachyonic fine-structure constant, cf. (4.7) and (5.22). The units $\hbar = c = 1$ can easily be restored. A spectral cutoff occurs at

$$\omega_{\max}(\gamma) = m_{\mathrm{t}}\left(\mu_{\mathrm{t}}\sqrt{\gamma^2-1} - \frac{1}{2}\frac{m_{\mathrm{t}}}{m}\gamma\right),$$
$$\mu_{\mathrm{t}} = \sqrt{1+\frac{1}{4}\frac{m_{\mathrm{t}}^2}{m^2}}. \tag{6.2}$$

Only frequencies in the range $0 \le \omega \le \omega_{\max}(\gamma)$ can be radiated by an inertial electron, the tachyonic spectral densities $p^{\mathrm{T,L}}(\omega,\gamma)$ being cut off at the break frequency $\omega_{\max}$. A positive $\omega_{\max}(\gamma)$ requires Lorentz factors exceeding the threshold μ_{t} [20].

We average the radiation densities (6.1) with a Boltzmann power-law distribution [32–34],

$$\mathrm{d}\rho_{\alpha,\beta}(\gamma) = A_{\alpha,\beta}\gamma^{-\alpha-1}\mathrm{e}^{-\beta\gamma}\sqrt{\gamma^2-1}\,\mathrm{d}\gamma, \tag{6.3}$$

where the normalization factor $A_{\alpha,\beta}$ is related to the electron number n_{e} by

$$n_e = A_{\alpha,\beta} K_{\alpha,\beta},$$
$$K_{\alpha,\beta} = \int_1^\infty \gamma^{-\alpha-1} e^{-\beta\gamma} \sqrt{\gamma^2-1}\, d\gamma. \quad (6.4)$$

The exponential cutoff with $\beta = m/(kT)$ determines the electron temperature, $kT[\mathrm{keV}] \approx 511/\beta$. A thermal Maxwell–Boltzmann distribution requires the electron index $\alpha = -2$.

The spectral average of the radiation densities (6.1) is carried out as [20, 21]

$$\langle p^{T,L}(\omega)\rangle_{\alpha,\beta} = \int_{\mu_t}^\infty p^{T,L}(\omega,\gamma)\theta\big(\omega_{\max}(\gamma)-\omega\big)\, d\rho_{\alpha,\beta}(\gamma), \quad (6.5)$$

where θ is the Heaviside step function. The spectral range of densities (6.1) is bounded by $\omega_{\max}$ in (6.2), so that the solution of $\omega = \omega_{\max}(\hat\gamma)$ defines the minimal electronic Lorentz factor for radiation at this frequency ,

$$\hat\gamma(\omega) = \mu_t\sqrt{\hat\omega^2+1} + \frac{1}{2}\frac{m_t}{m}\hat\omega, \quad (6.6)$$

where $\hat\omega = \omega/m_t$. The average (6.5) can be reduced to the spectral functions

$$B^{T,L}(\omega,\gamma_1) = \frac{1}{A_{\alpha,\beta}\alpha_t}\int_{\gamma_1}^\infty p^{T,L}(\omega,\gamma)\, d\rho_{\alpha,\beta}(\gamma), \quad (6.7)$$

so that

$$\langle p^{T,L}(\omega)\rangle_{\alpha,\beta} = A_{\alpha,\beta}\alpha_t B^{T,L}\big(\omega,\hat\gamma(\omega)\big). \quad (6.8)$$

The superscripts T and L denote the transversal and longitudinal radiation components. Performing the integration (6.7), we find

$$\begin{aligned} B^{T,L}(\omega,\gamma_1) &= \frac{m_t}{\beta^2\gamma_1^{\alpha+1}}\big(\hat\omega^2+1\big)^{\sigma-1}\hat\omega^{1-2\sigma} \\ &\quad\times\Big\{\Big[(1+\alpha)\alpha + (1+\alpha)\beta\frac{m_t}{m}\hat\omega \\ &\quad - \beta^2\big(\hat\omega^2+1\big)\Delta^{T,L} - \frac{1}{4}\beta^2\frac{m_t^2}{m^2}\Big] \\ &\quad\times(\beta\gamma_1)^{\alpha+1}\Gamma(-\alpha-1,\beta\gamma_1) \\ &\quad - \Big(\alpha-\beta\gamma_1+\beta\frac{m_t}{m}\hat\omega\Big)e^{-\beta\gamma_1}\Big\}, \end{aligned} \quad (6.9)$$

with $\Delta^{T,L}$ as in (6.1). The unpolarized density $\langle p^{T+L}(\omega)\rangle_{\alpha,\beta}$ is obtained by adding the polarization components, $B^{T+L} = B^T + B^L$. In the following, we use keV units for the tachyon and electron mass as well as the radiated frequencies, so that ω stands for $\hbar\omega[\mathrm{keV}]$ and m_t for $m_t c^2[\mathrm{keV}]$; the spectral functions $B^{T,L}$ and $\langle p^{T,L}(\omega)\rangle_{\alpha,\beta}$ are in keV units accordingly.

The incomplete gamma function in (6.9) satisfies

$$\begin{aligned} &\Gamma(-\alpha-1,\beta\gamma_1) \\ &\quad = -(\alpha+2)\Gamma(-\alpha-2,\beta\gamma_1) + (\beta\gamma_1)^{-\alpha-2}e^{-\beta\gamma_1}, \end{aligned} \quad (6.10)$$

and is elementary for thermal Boltzmann averages with $\alpha = -2$. $B^{T,L}(\omega,\gamma_1)$ decays exponentially for $\beta\gamma_1 \gg 1$, and so does $B^{T,L}(\omega,\hat\gamma(\omega))$ for $\hat\omega\to\infty$, since $\Gamma(-\alpha-1,\beta\gamma_1) \sim (\beta\gamma_1)^{-\alpha-2}e^{-\beta\gamma_1}$. Thus we can define the cutoff frequency as $\hat\gamma(\omega_{\mathrm{cut}}) - \hat\gamma(0) = 1/\beta$ or $\omega_{\mathrm{cut}} = \omega_{\max}(\mu_t + 1/\beta)$, cf. (6.2) and (6.6). In the low-frequency limit, $\hat\omega\to 0$, we find the scaling $B^{T,L}(\omega,\hat\gamma(\omega)) \propto \hat\omega^{1-2\sigma}$. The dependence of the spectral functions $B^{T,L}$ on the fine-structure scaling exponent σ weakens at high energy $\omega \gg m_t$, but it shows in the soft γ-ray band relevant for GRB spectra, where it determines the initial rise of the flux densities (6.11); σ is usually (but not always) close to 0.5 [19, 35–37].

The spectral fits of GRB 930506, GRB 950425, and GRB 910503 in Figs. 1, 2 and 3 are based on the E^2-rescaled flux densities

$$\begin{aligned} &E^2\frac{dN^{T,L}}{dE}\big[\mathrm{keV\,cm^{-2}\,s^{-1}}\big] \\ &\quad = \omega[\mathrm{keV}]\frac{\langle p^{T,L}(\omega)\rangle_{\alpha,\beta}[\mathrm{keV}]}{4\pi d^2[\mathrm{cm}]\hbar[\mathrm{keV\,s}]}, \end{aligned} \quad (6.11)$$

where $E = \hbar\omega$ is the energy of the radiated tachyons, d the distance to the source, $\langle p^{T,L}(\omega)\rangle_{\alpha,\beta}$ the spectral average (6.5), and $\hbar[\mathrm{keV\,s}] \approx 6.582\times 10^{-19}$. We consider ultra-relativistic multi-component plasmas in the collisionless regime [38], in stationary nonequilibrium described by the power-law densities (6.3); the fits are performed with the unpolarized flux density $dN^{T+L} = dN^T + dN^L$ (denoted by T + L in the figures, cf. the caption to Fig. 1) of plasma components ρ_i specified by the electronic power-law distributions in Table 1. We substitute the averaged density (6.8) into (6.11), and replace $A_{\alpha,\beta}\alpha_t/d^2$ by a fitting parameter $\hat n$ determined by the flux amplitude,

$$\begin{aligned} \frac{\hat n[\mathrm{keV\,cm^{-2}\,s^{-1}}]}{K_{\alpha,\beta}m_t^2[\mathrm{keV}]} &= \frac{A_{\alpha,\beta}\alpha_t}{4\pi d^2[\mathrm{cm}]\hbar[\mathrm{keV\,s}]} \\ &\approx 1.270\times 10^{-32}\frac{A_{\alpha,\beta}\alpha_t}{d^2[\mathrm{Mpc}]}. \end{aligned} \quad (6.12)$$

The GRB distances are estimated by $d \sim cz/H_0$, with the Hubble distance $c/H_0 \approx 4.41$ Gpc (that is, $h_0 \approx 0.68$). Hence, $d[\mathrm{Gpc}] \approx 4.41z$, so that we find the electron number of the source plasma as $n_e \approx 1.53\times 10^{39} z^2\hat n/(\alpha_t m_t^2)$. Estimates of the asymptotic fine-structure constant $\alpha_q(\omega\to\infty) \sim \alpha_t$ are obtained from the tachyonic luminosity of the GRB plasma, cf. Sect. 7. The redshifts of the GRBs depicted

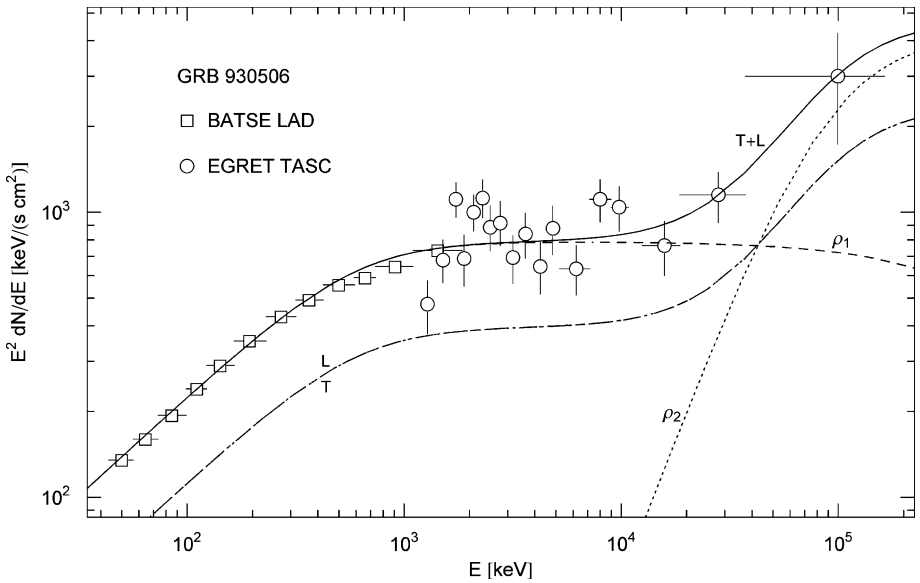

Fig. 1 Spectral map of γ-ray burst GRB 930506. BATSE and EGRET data points from Ref. [19]. The solid line T + L depicts the unpolarized differential tachyon flux $\mathrm{d}N^{\mathrm{T+L}}/\mathrm{d}E$, obtained by adding the flux densities $\rho_{1,2}$ radiated by an ultra-relativistic two-component plasma, and rescaled with E^2 for better visibility of the spectral curvature, cf. (6.11). The transversal and longitudinal flux densities $\mathrm{d}N^{\mathrm{T,L}}/\mathrm{d}E$ add up to the total unpolarized flux, $\mathrm{T} + \mathrm{L} = \rho_1 + \rho_2$. The exponential decay of the flux components $\rho_{1,2}$ sets in at about $E_{\mathrm{cut}} = \hbar\omega_{\max}(1/\beta + \mu_{\mathrm{t}})$, cf. (6.2) and after (6.10). The low-energy flux ρ_1 is fitted with the tachyon–electron mass ratio $m_{\mathrm{t}}/m \approx 1.2$, cf. Table 1, and the cutoff energy $E_{\mathrm{cut}} \approx 390$ MeV. The least-squares fit is performed with the unpolarized flux T + L, and subsequently split into transversal and longitudinal components

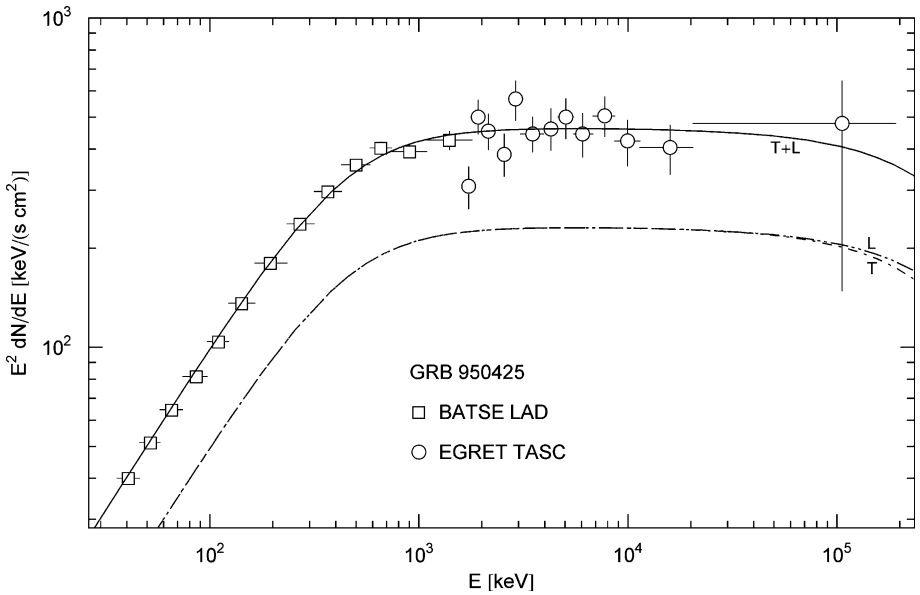

Fig. 2 Spectral map of GRB 950425. Flux data from Ref. [19], notation as in Fig. 1. T and L stand for the transversal and longitudinal flux components, and $\mathrm{T} + \mathrm{L} = \rho_1$ labels the unpolarized flux generated by a one-component electron plasma. The tachyon–electron mass ratio is $m_{\mathrm{t}}/m \approx 0.90$, and the tachyonic flux density T + L is exponentially cut at $E_{\mathrm{cut}} \approx 260$ MeV. The thermodynamic parameters and the tachyonic luminosity of the source plasma are recorded in Table 2

in Figs. 1–3 are unknown. The distance estimates do not affect the spectral fits but the luminosity, electron number, and internal energy of the source plasma, which scale with the squared redshift, assuming the above linear redshift–distance relation, cf. Table 2. The high-energy component ρ_2 of GRB 930506 in Fig. 1 does not imply a small redshift, as there is no intergalactic absorption of the tachyon flux by the cosmic background light [39, 40].

Table 1 Electron distributions ρ_i generating the tachyonic flux densities of the γ-ray bursts in Figs. 1–3. The components $\rho_{1,2}$ of the source plasma are specified by electronic power-law densities with electron index α and cutoff parameter β in the Boltzmann factor, cf. (6.3). m_t is the mass parameter of the superluminal modes, and σ the scaling exponent of the frequency-dependent tachyonic fine-structure constant, cf. (4.7). The scale factor $\hat{n}$ determining the amplitude of the superluminal flux is defined in (6.12). kT is the temperature of the plasma components, cf. after (6.4). As for GRB 930506 in Fig. 1, the temperature estimate of the high-energy component ρ_2 is tentative, owing to lack of flux data above 100 MeV

GRB	m_t (keV)	σ	α	β	$\hat{n}$ (keV cm^{-2} s^{-1})	kT (MeV)
930506						
ρ_1	600	0.65	−2	8.76×10^{-4}	396	5.83×10^2
ρ_2	9.0×10^4	0	−2	1.31×10^{-6}	2.11×10^3	3.90×10^5
950425						
ρ_1	460	0.5	−2	1.15×10^{-3}	233	4.44×10^2
910503						
ρ_1	410	0.55	0	2.41×10^{-2}	227	21.2

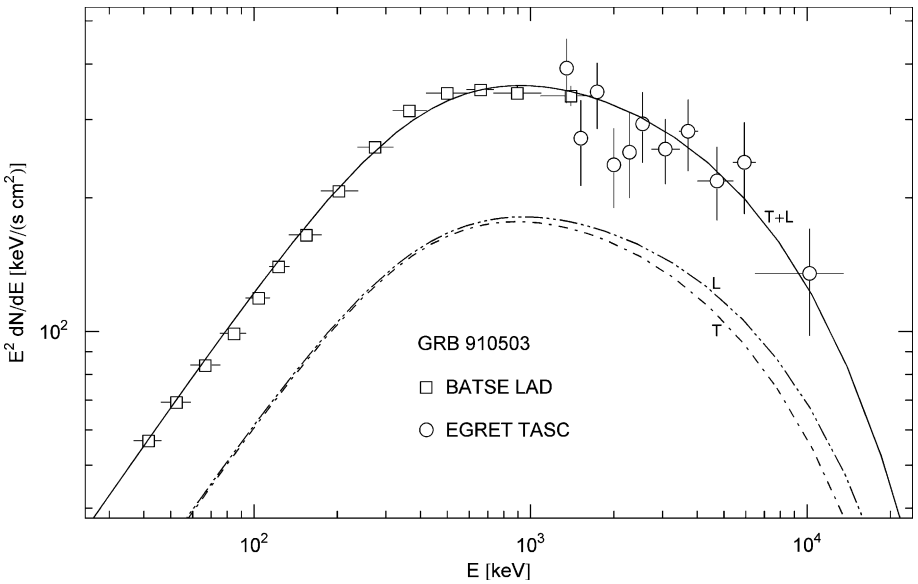

Fig. 3 Spectral map of GRB 910503. Flux points from Ref. [19], notation as in Figs. 1 and 2. The cutoff energy of the tachyonic flux density $\rho_1 = \mathrm{T} + \mathrm{L}$ is $E_\mathrm{cut} \approx 12$ MeV, with $m_\mathrm{t}/m \approx 0.80$. The superluminal flux is radiated by a nonthermal single-component plasma, cf. Tables 1 and 2

7 Tachyonic power transversally and longitudinally radiated

7.1 Radiant power of ultra-relativistic inertial electrons

The power radiated by an electron in uniform motion is $P^{\mathrm{T,L}} = \int_0^{\omega_\mathrm{max}} p^{\mathrm{T,L}} \mathrm{d}\omega$, with spectral density $p^{\mathrm{T,L}}(\omega, \gamma)$ in (6.1) and cutoff frequency $\omega_\mathrm{max}(\gamma)$ in (6.2) [20, 41]. When deriving the ultra-relativistic ($\gamma \gg 1$) asymptotics of $P^{\mathrm{T,L}}$, it is convenient to rewrite the radiation density (6.1) as

$$p^{\mathrm{T,L}}(\omega, \gamma) = \frac{\alpha_\mathrm{t} m_\mathrm{t} c^2}{\gamma\sqrt{\gamma^2 - 1}} \Bigg[\left(\gamma^2 - \frac{1}{4}\frac{m_\mathrm{t}^2}{m^2}\right) q_{0,0}(\hat{\omega}) - \frac{m_\mathrm{t}}{m}\gamma q_{1,0}(\hat{\omega}) - \Delta^{\mathrm{T,L}} q_{0,1}(\hat{\omega}) \Bigg], \tag{7.1}$$

where we restored dimensions and defined

$$q_{k,n}(\hat{\omega}) = \hat{\omega}^{1-2\sigma+k}\left(\hat{\omega}^2 + 1\right)^{\sigma-1+n}, \quad \hat{\omega} = \frac{\hbar\omega}{m_\mathrm{t} c^2}. \tag{7.2}$$

The power radiated in transversal (T) and longitudinal (L) polarization is assembled as

$$\begin{aligned} P^{\mathrm{T,L}}(\gamma) &= \frac{m_\mathrm{t} c^2}{\hbar} \int_0^{\hat{\omega}_\mathrm{max}(\gamma)} p^{\mathrm{T,L}}(\omega, \gamma)\, \mathrm{d}\hat{\omega} \\ &= \frac{\alpha_\mathrm{t}}{\gamma\sqrt{\gamma^2 - 1}} \frac{m_\mathrm{t}^2 c^4}{\hbar} \Bigg[\left(\gamma^2 - \frac{1}{4}\frac{m_\mathrm{t}^2}{m^2}\right) A_{0,0}\big(\hat{\omega}_\mathrm{max}(\gamma)\big) \\ &\quad - \frac{m_\mathrm{t}}{m}\gamma A_{1,0}\big(\hat{\omega}_\mathrm{max}(\gamma)\big) \\ &\quad - \Delta^{\mathrm{T,L}} A_{0,1}\big(\hat{\omega}_\mathrm{max}(\gamma)\big) \Bigg], \end{aligned} \tag{7.3}$$

Table 2 Tachyonic luminosity, electron number, and internal energy of the GRB source plasma. $\langle P^{\mathrm{T,L}}\rangle_{\alpha,\beta}$ denotes the power transversally and longitudinally radiated, cf. (7.21). α_{t} is the tachyonic fine-structure constant in the high-frequency limit, cf. (7.22), estimated from the burst duration τ_0 [19]. n_{e} is the electron count, cf. after (6.12), and U the internal energy, cf. after (7.24), of the respective plasma component ρ_i, cf. the caption to Table 1. The tachyonic power, electron number, and energy stored in the electron gas scale $\propto z^2$; we list these quantities at $z = 1$, since redshift estimates are not available for the GRBs in Figs. 1–3

GRB	τ_0(s)	$\langle P^{\mathrm{T}}\rangle_{\alpha,\beta}/z^2$ (erg/s)	$\langle P^{\mathrm{L}}\rangle_{\alpha,\beta}/z^2$ (erg/s)	α_{t}	n_{e}/z^2	U/z^2 (erg)
930506	65.6					
ρ_1		1.16×10^{52}	1.17×10^{52}	3.08×10^{-21}	5.48×10^{56}	1.53×10^{54}
ρ_2		6.71×10^{52}	6.52×10^{52}	8.56×10^{-23}	4.66×10^{54}	8.68×10^{54}
950425	131					
ρ_1		6.29×10^{51}	6.40×10^{51}	2.16×10^{-21}	7.81×10^{56}	1.66×10^{54}
910503	98.3					
ρ_1		2.61×10^{51}	2.74×10^{51}	1.35×10^{-22}	1.53×10^{58}	5.26×10^{53}

where we use the shortcut

$$A_{k,n}(\hat{\omega}) = \int_0^{\hat{\omega}} q_{k,n}(\hat{\omega})\,\mathrm{d}\hat{\omega}. \tag{7.4}$$

It is assumed that $\gamma > \mu_{\mathrm{t}}$, where μ_{t} is the electronic threshold Lorentz factor for superluminal radiation to occur, cf. (6.2). The total unpolarized power radiated is obtained by adding the polarization components, $P^{\mathrm{T+L}} = P^{\mathrm{T}} + P^{\mathrm{L}}$. For the integrals $A_{k,n}$ in (7.4) to converge at the lower integration boundary, $k > 2(\sigma - 1)$ is required; convergence of $P^{\mathrm{T,L}}$ is thus assured by $\sigma < 1$, which we henceforth assume, cf. after (4.11). The upper integration boundary in (7.3) is

$$\hat{\omega}_{\max}(\gamma) = \frac{\hbar\omega_{\max}}{m_{\mathrm{t}}c^2} = \mu_{\mathrm{t}}\sqrt{\gamma^2-1} - \frac{1}{2}\frac{m_{\mathrm{t}}}{m}\gamma. \tag{7.5}$$

To derive the $\hat{\omega}\to\infty$ asymptotics of the integrals $A_{k,n}(\hat{\omega})$ in (7.4), we note

$$\begin{aligned} &A_{k,n}(\hat{\omega}) = C_{k,n} - B_{k,n}(\hat{\omega}),\\ &B_{k,n}(\hat{\omega}) = \int_{\hat{\omega}}^{\infty} q_{k,n}(\hat{\omega})\,\mathrm{d}\hat{\omega}, \qquad C_{k,n} = \int_0^{\infty} q_{k,n}(\hat{\omega})\,\mathrm{d}\hat{\omega}. \end{aligned} \tag{7.6}$$

The integrals in (7.4) and (7.6) are representations of hypergeometric functions [42],

$$\begin{aligned} A_{k,n}(\hat{\omega}) &= \frac{\hat{\omega}^{2-2\sigma+k}}{2-2\sigma+k}\\ &\quad\times {}_2F_1\left(1-\sigma-n, 1-\sigma+\frac{k}{2}; 2-\sigma+\frac{k}{2}; -\hat{\omega}^2\right), \end{aligned} \tag{7.7}$$

$$\begin{aligned} B_{k,n}(\hat{\omega}) &= -\frac{\hat{\omega}^{k+2n}}{k+2n}\\ &\quad\times {}_2F_1\left(1-\sigma-n, -\frac{k}{2}-n; 1-\frac{k}{2}-n; -\frac{1}{\hat{\omega}^2}\right), \end{aligned} \tag{7.8}$$

$$C_{k,n} = \frac{\Gamma(1-\sigma+k/2)\Gamma(-k/2-n)}{2\Gamma(1-\sigma-n)}, \tag{7.9}$$

which can also be used for noninteger k and n, in case that analytic continuation is needed. In leading order, the $\hat{\omega}\to\infty$ asymptotics of integrals (7.4) is thus $A_{k,n}(\hat{\omega}) \sim C_{k,n}$ for $k+2n<0$, and $A_{k,n}(\hat{\omega}) \sim \hat{\omega}^{k+2n}/(k+2n)$ for $k+2n>0$, as well as $A_{k,n}(\hat{\omega}) \sim \log\hat{\omega}$ for $k+2n=0$. If $n = 1-\sigma+j$ with integer $j\geq 0$, then ${}_2F_1$ in (7.7) is a hypergeometric polynomial. If $k+2n = 2l$ with integer $l\geq 0$, we remove the singularities arising in the gamma functions and series coefficients by ε regularization, putting $k = 2(l-n)+\varepsilon$, so that

$$\begin{aligned} &C_{2(l-n)+\varepsilon,n}\\ &\quad= (1-\sigma-n)_l\frac{(-)^{l+1}}{l!}\left(\frac{1}{\varepsilon} + \frac{1}{2}\psi(1-\sigma-n+l)\right.\\ &\qquad\left. - \frac{1}{2}\psi(l+1) + \mathrm{O}(\varepsilon)\right), \end{aligned} \tag{7.10}$$

where ψ denotes the logarithmic derivative of the gamma function, and $(\alpha)_l$ is Pochhammer's symbol $\Gamma(\alpha+l)/\Gamma(\alpha)$. The same regularization applied to $B_{2(l-n)+\varepsilon,n}(\hat{\omega})$ in (7.8) gives

$$\begin{aligned} &B_{2(l-n)+\varepsilon,n}(\hat{\omega})\\ &\quad= \frac{(-)^{l+1}}{l!}(1-\sigma-n)_l\left(\frac{1}{\varepsilon} + \log\hat{\omega}\right)\\ &\qquad+ \frac{\hat{\omega}^{2l}}{2}\sum_{\substack{j=0\\ j\neq l}}^{\infty}\frac{(1-\sigma-n)_j(-)^j}{(j-l)\,j!\hat{\omega}^{2j}} + \mathrm{O}(\varepsilon). \end{aligned} \tag{7.11}$$

In this way, we find $A_{2(l-n),n}(\hat{\omega})$ and in particular $A_{0,0}(\hat{\omega})$ and $A_{0,1}(\hat{\omega})$ in (7.3), since the ε poles cancel in $C_{2(l-n)+\varepsilon,n} - B_{2(l-n)+\varepsilon,n}(\hat{\omega})$, so that we can perform the limit $\varepsilon\to 0$.

Expanding $\hat{\omega}_{\max}(\gamma \gg 1)$ in (7.5),

$$\hat{\omega}_{\max} = \kappa_{\mathrm{t}}\gamma\left(1 - \frac{\mu_{\mathrm{t}}}{2\kappa_{\mathrm{t}}}\frac{1}{\gamma^2} + \mathrm{O}\left(\frac{1}{\gamma^4}\right)\right),$$
$$\kappa_{\mathrm{t}} := \sqrt{1 + \frac{1}{4}\frac{m_{\mathrm{t}}^2}{m^2}} - \frac{1}{2}\frac{m_{\mathrm{t}}}{m}, \tag{7.12}$$

and substituting this into (7.8)–(7.11), we obtain the ultra-relativistic expansions of the integrals $A_{k,n}(\hat{\omega}_{\max}(\gamma))$ in (7.3),

$$A_{0,0}(\hat{\omega}_{\max}) = \log(\kappa_{\mathrm{t}}\gamma) + \frac{1}{2}\psi(1) - \frac{1}{2}\psi(1-\sigma) + \left(\frac{1-\sigma}{2\kappa_{\mathrm{t}}^2} - \frac{\mu_{\mathrm{t}}}{2\kappa_{\mathrm{t}}}\right)\frac{1}{\gamma^2} + \mathrm{O}\left(\frac{1}{\gamma^4}\right),$$
$$A_{1,0}(\hat{\omega}_{\max}) = \kappa_{\mathrm{t}}\gamma - \sqrt{\pi}\frac{\Gamma(3/2-\sigma)}{\Gamma(1-\sigma)} + \left(\frac{1-\sigma}{\kappa_{\mathrm{t}}} - \frac{\mu_{\mathrm{t}}}{2}\right)\frac{1}{\gamma} + \mathrm{O}\left(\frac{1}{\gamma^3}\right), \tag{7.13}$$
$$A_{0,1}(\hat{\omega}_{\max}) = \frac{\kappa_{\mathrm{t}}^2}{2}\gamma^2 + \sigma\log(\kappa_{\mathrm{t}}\gamma) + \frac{\sigma}{2}\psi(2) - \frac{\sigma}{2}\psi(1-\sigma) - \frac{\mu_{\mathrm{t}}\kappa_{\mathrm{t}}}{2} + \mathrm{O}\left(\frac{1}{\gamma^2}\right).$$

The radiant power $P^{\mathrm{T,L}}(\gamma \gg 1)$ thus reads

$$P^{\mathrm{T,L}}(\gamma) = \frac{\alpha_{\mathrm{t}} m_{\mathrm{t}}^2 c^4/\hbar}{\gamma\sqrt{\gamma^2-1}}\left(\gamma^2(\log\gamma + a_2) + \gamma a_1 + a_{\mathrm{sing}}\log\gamma + a_0 + \mathrm{O}\left(\frac{1}{\gamma^2}\right)\right), \tag{7.14}$$

where $m_{\mathrm{t}}^2 c^4 \hbar^{-1}[\mathrm{keV/s}] \approx 1.519 \times 10^{18} m_{\mathrm{t}}^2[\mathrm{keV}]$. Estimates of the tachyonic fine-structure constant α_{t} of GRB electron plasmas are given in Table 2. The series coefficients in (7.14) are

$$a_2 = \frac{1}{2}\psi(1) - \frac{1}{2}\psi(1-\sigma) + \log\kappa_{\mathrm{t}} - \frac{1}{2}\Delta^{\mathrm{T,L}}\kappa_{\mathrm{t}}^2 - \frac{m_{\mathrm{t}}}{m}\kappa_{\mathrm{t}},$$
$$a_1 = \sqrt{\pi}\frac{\Gamma(3/2-\sigma)}{\Gamma(1-\sigma)}\frac{m_{\mathrm{t}}}{m}, \qquad a_{\mathrm{sing}} = -\sigma\Delta^{\mathrm{T,L}} - \frac{1}{4}\frac{m_{\mathrm{t}}^2}{m^2},$$
$$a_0 = \frac{1-\sigma}{2\kappa_{\mathrm{t}}^2} - \frac{\mu_{\mathrm{t}}}{2\kappa_{\mathrm{t}}} + \frac{1}{2}\Delta^{\mathrm{T,L}}\big(\sigma\psi(1-\sigma) - \sigma\psi(2) + \mu_{\mathrm{t}}\kappa_{\mathrm{t}} - 2\sigma\log\kappa_{\mathrm{t}}\big) + \frac{m_{\mathrm{t}}}{m}\left(\frac{\mu_{\mathrm{t}}}{2} - \frac{1-\sigma}{\kappa_{\mathrm{t}}}\right) + \frac{1}{8}\frac{m_{\mathrm{t}}^2}{m^2}\big(\psi(1-\sigma) - \psi(1) - 2\log\kappa_{\mathrm{t}}\big). \tag{7.15}$$

$P^{\mathrm{T,L}}(\gamma)$ in (7.14) is the transversal/longitudinal tachyonic power radiated by an ultra-relativistic inertial electron. The power collectively radiated by the electrons of a burst plasma is discussed in the next subsection.

7.2 Tachyonic luminosity of GRB plasmas

The tachyonic power of an ultra-relativistic electron gas is found by averaging $P^{\mathrm{T,L}}(\gamma)$ in (7.3) over the electron density (6.3):

$$\big\langle P^{\mathrm{T,L}}\big\rangle_{\alpha,\beta} = \int_{\mu_{\mathrm{t}}}^{\infty} P^{\mathrm{T,L}}(\gamma)\,\mathrm{d}\rho_{\alpha,\beta}(\gamma),$$
$$\big\langle P^{\mathrm{T+L}}\big\rangle_{\alpha,\beta} = \big\langle P^{\mathrm{T}}\big\rangle_{\alpha,\beta} + \big\langle P^{\mathrm{L}}\big\rangle_{\alpha,\beta}. \tag{7.16}$$

The lower integration boundary μ_{t} is the threshold Lorentz factor in (6.2). The high-temperature asymptotics $\beta \ll 1$ of this average is derived in Appendix B. We find in leading order, cf. (B.3), (B.13), and (B.26),

$$\big\langle P^{\mathrm{T,L}}\big\rangle_{\alpha,\beta} \sim \frac{m_{\mathrm{t}}^2 c^4}{\hbar} n_{\mathrm{e}}\alpha_{\mathrm{t}}\left(\log\frac{1}{\beta} + \psi(1-\alpha) + a_2\right), \tag{7.17}$$

valid for electron indices $\alpha < 1$ and $\beta \to 0$. The constant a_2 defined in (7.15) depends on the tachyon–electron mass ratio m_{t}/m, the fine-structure scaling exponent σ, and the polarization $\Delta^{\mathrm{T,L}}$, cf. after (6.1); ψ denotes the psi function [42]. For electron indices $\alpha > 1$, the leading order of $\langle P^{\mathrm{T,L}}\rangle_{\alpha,\beta}$ is independent of β, cf. (B.5) and (B.26),

$$\big\langle P^{\mathrm{T,L}}\big\rangle_{\alpha,\beta} \sim \frac{m_{\mathrm{t}}^2 c^4}{\hbar}\frac{n_{\mathrm{e}}\alpha_{\mathrm{t}}}{c_{0,\alpha}}\big(f_{\alpha,\infty}^{\mathrm{T,L}} - g_{\alpha,\infty}^{\mathrm{T,L}} - h_{\alpha,\infty}^{\mathrm{T,L}}\big), \tag{7.18}$$

where the constants $(f,g,h)_{\alpha,\infty}^{\mathrm{T,L}}$ and $c_{0,\alpha}$ are listed in (B.6) and (B.27). The borderline case $\alpha = 1$ admits a logarithmic temperature dependence, and is assembled as

$$\big\langle P^{\mathrm{T,L}}\big\rangle_{1,\beta} \sim \frac{m_{\mathrm{t}}^2 c^4}{\hbar}\frac{n_{\mathrm{e}}\alpha_{\mathrm{t}}}{K_{1,\beta}}\big(P_{1,\beta}^{\mathrm{T,L}} - P_{1,\Lambda}^{\mathrm{T,L}} + f_{1,\Lambda}^{\mathrm{T,L}} - g_{1,\Lambda}^{\mathrm{T,L}} - h_{1,\Lambda}^{\mathrm{T,L}}\big), \tag{7.19}$$

with normalization $K_{1,\beta}$ in (B.28) and $\Lambda \to \infty$. The shortcuts $P_{1,\beta}^{\mathrm{T,L}}$, $P_{1,\Lambda}^{\mathrm{T,L}}$, and $(f,g,h)_{\alpha,\Lambda}^{\mathrm{T,L}}$ are defined in (B.6) and (B.24).

Alternatively, the power $\langle P^{\mathrm{T,L}}\rangle_{\alpha,\beta}$ can be calculated by first performing the average of $p^{\mathrm{T,L}}(\omega,\gamma)$ over the electron density as done in (6.5), and subsequently the frequency integration of $\langle p^{\mathrm{T,L}}(\omega)\rangle_{\alpha,\beta}$. This also allows us to estimate the power radiated in a finite frequency interval (ω_1,ω_2),

$$\big\langle P^{\mathrm{T,L}}\big\rangle_{\alpha,\beta}[\mathrm{keV/s}] = \frac{1}{\hbar[\mathrm{keV\,s}]}\int_{\omega_1}^{\omega_2}\big\langle p^{\mathrm{T,L}}(\omega)\big\rangle_{\alpha,\beta}\,\mathrm{d}\omega, \tag{7.20}$$

where we substitute $\langle p^{\mathrm{T,L}}(\omega)\rangle_{\alpha,\beta}$ as stated in (6.8) and (6.9), with integration boundaries $\omega_{1,2}$ in keV units. Integrating over the full frequency range, $\omega_1 = 0$, $\omega_2 = \infty$, we arrive at

$\langle P^{\mathrm{T,L}}\rangle_{\alpha,\beta}$ in (7.16), as we have only interchanged integrations. The integrand in (7.20) decays exponentially at high frequencies, cf. after (6.10). Convergence at the lower integration boundary $\omega_1 = 0$ requires $\sigma < 1$, cf. after (7.4). By making use of (6.8), we can write

$$\begin{aligned}&\big\langle P^{\mathrm{T,L}}\big\rangle_{\alpha,\beta}[\mathrm{keV/s}]\\&\quad= \frac{4\pi d^2[\mathrm{cm}]\hat{n}}{K_{\alpha,\beta} m_{\mathrm{t}}^2[\mathrm{keV}]}\int_{\omega_1}^{\omega_2} B^{\mathrm{T,L}}\big(\omega,\hat{\gamma}(\omega)\big)\,\mathrm{d}\omega,\end{aligned}\tag{7.21}$$

where $\hat{n}$ is the parameter $\hat{n}[\mathrm{keV\,cm^{-2}\,s^{-1}}]$ in (6.12) obtained from the spectral fit, and $d[\mathrm{cm}] \approx 3.086\times 10^{24} d[\mathrm{Mpc}]$, so that $4\pi d^2[\mathrm{cm}] \approx 2.33\times 10^{57} z^2$, cf. after (6.12). We also note $\langle P^{\mathrm{T,L}}\rangle_{\alpha,\beta}[\mathrm{erg/s}] \approx 1.602\times 10^{-9}\langle P^{\mathrm{T,L}}\rangle_{\alpha,\beta}[\mathrm{keV/s}]$. The total unpolarized power $\langle P^{\mathrm{T+L}}\rangle_{\alpha,\beta}$ is obtained by adding the polarization components, replacing $B^{\mathrm{T,L}}$ by $B^{\mathrm{T}} + B^{\mathrm{L}}$ in the integrand, cf. (6.9).

We identify the burst duration with the time scale $\tau_0 = U/\langle P^{\mathrm{T+L}}\rangle_{\alpha,\beta}$ in which the internal energy U of the electron gas is radiated off. We use $U[\mathrm{keV}] = n_{\mathrm{e}} m[\mathrm{keV}] u_\alpha(\beta)$, cf. (7.23), and $\langle P^{\mathrm{T+L}}\rangle_{\alpha,\beta}$ in (7.21) to estimate the asymptotic fine-structure constant from the burst duration,

$$\alpha_{\mathrm{t}} = \frac{m[\mathrm{keV}]\hbar[\mathrm{keV\,s}] K_{\alpha,\beta} u_\alpha(\beta)}{\tau_0[\mathrm{s}]\int_0^\infty B^{\mathrm{T+L}}(\omega,\hat{\gamma}(\omega))\,\mathrm{d}\omega}.\tag{7.22}$$

The electron number n_{e} drops out, since both U and $\langle P^{\mathrm{T+L}}\rangle_{\alpha,\beta}$ scale linearly with n_{e}. Once α_{t} is known, we can calculate n_{e} as indicated after (6.12).

The high-temperature limit of the internal energy $U = n_{\mathrm{e}} m u_\alpha(\beta)$ of the GRB plasma differs qualitatively in different α ranges [32]:

$$\begin{aligned}&u_{\alpha<1} \sim \frac{1-\alpha}{\beta},\qquad u_{1<\alpha<2} \sim \frac{2\alpha}{\sqrt{\pi}}\frac{\Gamma(\alpha/2)\Gamma(2-\alpha)}{\Gamma((\alpha-1)/2)}\beta^{\alpha-2},\\&u_{\alpha>2} \sim \frac{\Gamma(\alpha/2+1)\Gamma(\alpha/2-1)}{\Gamma((\alpha+1)/2)\Gamma((\alpha-1)/2)}.\end{aligned}\tag{7.23}$$

The leading order of $u_{\alpha>2}$ is independent of β, so that the energy stored in an ultra-relativistic electron plasma with electron index $\alpha > 2$ admits a finite high-temperature limit. Integer electron indices require special treatment due to a logarithmic temperature dependence,

$$\begin{aligned}u_{\alpha=1} &\sim \frac{1}{\beta}\frac{1}{\log(2/\beta)-\gamma_{\mathrm{E}}-1},\\ u_{\alpha=2} &\sim \frac{4}{\pi}\left(\log\frac{2}{\beta}-\gamma_{\mathrm{E}}-1\right),\end{aligned}\tag{7.24}$$

where γ_{E} denotes the Euler constant. The energy estimates of the plasma components $\rho_{1,2}$ in Table 2 are based on $U[\mathrm{erg}] \sim 8.187\times 10^{-7} n_{\mathrm{e}}(1-\alpha)/\beta$, valid for $\alpha < 1$.

Instead of (7.21), we can use the asymptotic radiant power in (7.17)–(7.19) to estimate α_{t}. For electron indices $\alpha < 1$, we balance $\langle P^{\mathrm{T,L}}\rangle_{\alpha,\beta}$ in (7.17) with $n_{\mathrm{e}} m u_{\alpha<1}/\tau_0$ to find

$$\begin{aligned}\alpha_{\mathrm{t}} \sim{}& \frac{1}{\tau_0}\frac{\hbar}{mc^2}\frac{m^2}{m_{\mathrm{t}}^2}\frac{1}{\beta}\\&\times\frac{1-\alpha}{a_{2,\mathrm{T}}+a_{2,\mathrm{L}}+2\psi(1-\alpha)-2\log\beta},\end{aligned}\tag{7.25}$$

where $a_{2,\mathrm{T}} + a_{2,\mathrm{L}}$ stems from the summation over the polarization components in (7.17). We note $\hbar/(mc^2) \approx 1.288\times 10^{-21}\mathrm{s}$, and the burst duration τ_0 is typically of the order of 100 s.

8 Conclusion

We have studied γ-ray burst spectra by means of tachyonic spectral fits, and obtained estimates of the thermodynamic parameters of the electron plasma generating the superluminal radiation, cf. Tables 1 and 2. The low-frequency scaling of the averaged spectral densities is determined by the scaling exponent σ of the tachyonic fine-structure constant, cf. (4.7) and after (6.10). This exponent can therefore be extracted from the low-energy slope of the tachyonic flux densities in Figs. 1–3. The latter are peaked at a moderate multiple of the tachyon mass, which allows one to estimate the mass parameter m_{t} of the tachyonic modes radiated by the respective plasma component, cf. Table 1. The energy carried by the radiation modes is related to the tachyonic Lorentz factor $\gamma_{\mathrm{t}} = (\upsilon_{\mathrm{t}}^2 - 1)^{-1/2}$ by $\omega = m_{\mathrm{t}}\gamma_{\mathrm{t}}$. For instance, in the case of GRB 910503 in Fig. 3, the rescaled flux density peaks at about 1 MeV, so that the tachyon mass of 0.4 MeV implies a superluminal speed of $\upsilon_{\mathrm{t}}/c \approx 1.1$ at the peak frequency. The exponential cutoff of the flux density happens at $\omega_{\mathrm{cut}} \approx m_{\mathrm{t}}/\beta$, cf. the caption to Fig. 1, which provides an estimate of the plasma temperature.

In Sects. 2, 3, and 5, we investigated superluminal energy transfer and tachyonic wave propagation in electron plasmas, derived the dispersion relations for longitudinal and transversal tachyons, and analyzed conductivity properties such as relaxation times and extinction coefficients. We have studied the nonlocal interaction of the plasma current with the superluminal radiation field, in particular the long-range dispersion generated by the varying coupling constant, cf. Sect. 4 and Appendix A. We discussed the tachyonic power radiated by ultra-relativistic electrons, both individually and averaged over the plasma components, cf. Sect. 7 and Appendix B, and disentangled the transversal and longitudinal radiation components in the spectral maps, cf. Figs. 1–3. In Table 2, we estimated the scaling amplitude of the tachyonic fine-structure constant from the burst duration, as well as the tachyonic luminosity and internal energy of the burst plasma.

The spectrum of GRB 930506 in Fig. 1 is fitted with a two-component plasma, and the corresponding flux components have been resolved in the spectral map, so that the parameters of each plasma component can be extracted from the spectral fit. The radiation mechanism is the same for both components, cf. Sect. 6, but the high-energy component is radiated at a higher temperature and with a larger mass parameter, cf. Table 1. Extended spectral plateaus like that of GRB 950425 in Fig. 2, ranging over two orders in frequency, are a common occurrence in γ-ray spectra of Galactic sources [32, 33, 43] as well as in the thermal spectra of TeV blazars [26, 27], and tachyonic flux densities are quite capable of reproducing these plateaus.

Acknowledgements The author acknowledges the support of the Japan Society for the Promotion of Science. The hospitality and stimulating atmosphere of the Centre for Nonlinear Dynamics, Bharathidasan University, Trichy, and the Institute of Mathematical Sciences, Chennai, are likewise gratefully acknowledged.

Appendix A: Time evolution of the nonlocal charge density

The regular part of the extended charge density $\rho_\Omega(\mathbf{x},t)$ in (4.15) and (4.16) is defined by $\Omega_{\rm reg}(t)$, which admits the integral representation

$$\Omega_{\rm reg}(t)=\frac{1}{\pi}\,\mathrm{Re}\,\Xi,$$
$$\Xi(t)=\int_0^\infty\big(\hat\Omega(\omega)-1\big)\exp(-\mathrm{i}\omega t)\,\mathrm{d}\omega, \tag{A.1}$$

with $\hat\Omega=(1+m_\mathrm{t}^2/\omega^2)^{\sigma/2}$, cf. (4.7). Throughout this appendix, the time variable can be replaced by $t-z/\upsilon$ without further changes, cf. (4.16), which allows us to estimate the dispersion from the time asymptotics of $\Omega_{\rm reg}(t)$. To derive the latter, we split integral Ξ into a low- and high-frequency part,

$$\begin{aligned}\Xi_0&:=\int_0^\Lambda(\hat\Omega-1)\exp(-\mathrm{i}\omega t)\,\mathrm{d}\omega,\\ \Xi_\infty&:=\int_\Lambda^\infty(\hat\Omega-1)\exp(-\mathrm{i}\omega t)\,\mathrm{d}\omega,\end{aligned} \tag{A.2}$$

where Λ is a conveniently chosen cutoff parameter.

A.1 Large-t asymptotics of the regular charge distribution

To calculate the asymptotic series of $\Omega_{\rm reg}(t\to\infty)$, we use a cutoff $\Lambda<m_\mathrm{t}$ in (A.2). First, we consider Ξ_0, expand $\hat\Omega$ in ascending powers of ω^2/m_t^2, and employ term-by-term integration to find

$$\begin{aligned}\Xi_0&\sim-\int_0^\Lambda\exp(-\mathrm{i}\omega t)\,\mathrm{d}\omega\\&\quad+m_\mathrm{t}\sum_{k=0}^\infty\binom{\sigma/2}{k}(\Lambda/m_\mathrm{t})^{2k+1-\sigma}\frac{\gamma(2k+1-\sigma,\mathrm{i}\Lambda t)}{(\mathrm{i}\Lambda t)^{2k+1-\sigma}}.\end{aligned} \tag{A.3}$$

On substituting $\gamma(\alpha,\mathrm{i}\Lambda t)=\Gamma(\alpha)-\Gamma(\alpha,\mathrm{i}\Lambda t)$, where $\gamma(\alpha,z)$ and $\Gamma(\alpha,z)$ are incomplete gamma functions [42], we obtain

$$\Xi_0\sim\frac{\exp(-\mathrm{i}\Lambda t)-1}{\mathrm{i}t}+\Xi_{0,1}+\Xi_{0,2}, \tag{A.4}$$

$$\Xi_{0,1}:=m_\mathrm{t}\sum_{k=0}^\infty\binom{\sigma/2}{k}\frac{\Gamma(2k+1-\sigma)}{(\mathrm{i}m_\mathrm{t}t)^{2k+1-\sigma}}, \tag{A.5}$$

$$\begin{aligned}\Xi_{0,2}&:=-\Lambda\sum_{k=0}^\infty\binom{\sigma/2}{k}(\Lambda/m_\mathrm{t})^{2k-\sigma}\\&\quad\times\frac{\Gamma(2k+1-\sigma,\mathrm{i}\Lambda t)}{(\mathrm{i}\Lambda t)^{2k+1-\sigma}},\end{aligned} \tag{A.6}$$

where

$$\begin{aligned}\binom{\sigma/2}{k}&=(-)^k\frac{\Gamma(k-\sigma/2)}{k!\Gamma(-\sigma/2)}\\&=\frac{1}{k!}\frac{\sigma}{2}\left(\frac{\sigma}{2}-1\right)\cdots\left(\frac{\sigma}{2}-k+1\right).\end{aligned} \tag{A.7}$$

In (A.6), we substitute the asymptotic series of the incomplete gamma function,

$$\frac{\Gamma(\alpha,\mathrm{i}\Lambda t)}{(\mathrm{i}\Lambda t)^\alpha}\sim\frac{\exp(-\mathrm{i}\Lambda t)}{\mathrm{i}\Lambda t}\sum_{n=0}^\infty\frac{(-)^n}{(\mathrm{i}\Lambda t)^n}\frac{\Gamma(1-\alpha+n)}{\Gamma(1-\alpha)}, \tag{A.8}$$

and interchange the summations, to find

$$\Xi_{0,2}\sim-\frac{\exp(-\mathrm{i}\Lambda t)}{\mathrm{i}t}\sum_{n=0}^\infty\frac{c_n(\Lambda/m_\mathrm{t})}{(\mathrm{i}\Lambda t)^n}, \tag{A.9}$$

with coefficients

$$\begin{aligned}c_n(x)&=(-)^n\sum_{k=0}^\infty\binom{\sigma/2}{k}\frac{\Gamma(\sigma-2k+n)}{\Gamma(\sigma-2k)}x^{2k-\sigma}\\&=x^n\frac{\mathrm{d}^n}{\mathrm{d}x^n}\big[\big(1+x^2\big)^{\sigma/2}x^{-\sigma}\big].\end{aligned} \tag{A.10}$$

The series in (A.10) is summed by substitution of the derivatives $(x^\alpha)^{(n)}=(-)^nx^{\alpha-n}(-\alpha)_n$ at $\alpha=2k-\sigma$, where $(-\alpha)_n$ is Pochhammer's symbol $\Gamma(-\alpha+n)/\Gamma(-\alpha)$.

As for the high-frequency part Ξ_∞ in (A.2), we note that $\hat\Omega(\omega)-1$ and all its derivatives vanish at infinity, and apply iterated partial integration to find the asymptotic series

$$\Xi_\infty \sim \exp(-\mathrm{i}\Lambda t)\sum_{n=0}^{\infty}\frac{1}{(\mathrm{i}t)^{n+1}}\frac{\mathrm{d}^n}{\mathrm{d}\Lambda^n}\big(\hat\Omega(\Lambda)-1\big)$$
$$= -\frac{\exp(-\mathrm{i}\Lambda t)}{\mathrm{i}t}\left(1-\sum_{n=0}^{\infty}\frac{c_n}{(\mathrm{i}\Lambda t)^n}\right), \tag{A.11}$$
$$c_n := \Lambda^n\frac{\mathrm{d}^n}{\mathrm{d}\Lambda^n}\big(1+m_\mathrm{t}^2/\Lambda^2\big)^{\sigma/2}.$$

The coefficients c_n apparently coincide with $c_n(\Lambda/m_\mathrm{t})$ in (A.10). We assemble $\Xi = \Xi_0 + \Xi_\infty$ by way of (A.4), (A.5), (A.9), and (A.11),

$$\Xi \sim \frac{\mathrm{i}}{t} + m_\mathrm{t}\sum_{k=0}^{\infty}\binom{\sigma/2}{k}\frac{\Gamma(2k+1-\sigma)}{(\mathrm{i}m_\mathrm{t}t)^{2k+1-\sigma}}. \tag{A.12}$$

$\sigma < 1$ is required for integral (A.1) to converge. There are no oscillating terms, as the series in (A.9) and (A.11) cancel each other. We may split Ξ into a real and imaginary part,

$$\mathrm{Re}\,\Xi \sim \sin\left(\frac{\pi}{2}\sigma\right)S_\infty,$$
$$\mathrm{Im}\,\Xi \sim \frac{1}{t} - \mathrm{sign}(t)\cos\left(\frac{\pi}{2}\sigma\right)S_\infty, \tag{A.13}$$
$$S_\infty := \frac{m_\mathrm{t}\Gamma(1-\sigma)}{(m_\mathrm{t}|t|)^{1-\sigma}}\sum_{k=0}^{\infty}\binom{\sigma/2}{k}\frac{(-)^k(1-\sigma)_{2k}}{(m_\mathrm{t}t)^{2k}},$$

where we use the Pochhammer symbol

$$(1-\sigma)_{2k} := \frac{\Gamma(2k+1-\sigma)}{\Gamma(1-\sigma)}$$
$$= (1-\sigma)(2-\sigma)\cdots(2k-\sigma). \tag{A.14}$$

The leading order of series S_∞ is always positive, so that the sign of $\mathrm{Re}\,\Xi$ is determined in this limit by the sine factor in (A.13). We note that $\mathrm{Im}\,\Xi \sim 1/t$ for negative odd integer $\sigma = -2n-1$, $n = 0, 1, 2, \ldots$, irrespectively of n, so that the difference between different $\mathrm{Im}\,\Xi_{\sigma=-2n-1}$ is exponentially small. Likewise, the asymptotic expansion of $\mathrm{Re}\,\Xi$ vanishes for $\sigma = -2n$, since, at negative even integer σ, the real part of the integral (which is elementary) decays $\propto\exp(-m_\mathrm{t}|t|)$, and exponentially small terms are not included in the expansion (A.12).

A.2 Ascending time series of the extended charge density

To derive the series expansion of $\Omega_\mathrm{reg}(t\to 0)$ in ascending powers of t, cf. (A.1), we start with the truncated integral Ξ_0 in (A.2), and choose a cutoff $\Lambda > m_\mathrm{t}$. Expanding the exponential, we arrive at the integrals

$$K_n = \int_0^\Lambda \hat\Omega(\omega)\omega^n\,\mathrm{d}\omega,$$
$$\hat\Omega(\omega) = \frac{m_\mathrm{t}^\sigma}{\omega^\sigma}\big(1+\omega^2/m_\mathrm{t}^2\big)^{\sigma/2}, \tag{A.15}$$

which represent hypergeometric functions,

$$K_n = m_\mathrm{t}^{n+1}\frac{(\Lambda/m_\mathrm{t})^{n-\sigma+1}}{n-\sigma+1}$$
$$\times\,{}_2F_1\left(-\frac{\sigma}{2},\frac{n-\sigma+1}{2};\frac{n-\sigma+3}{2};-\frac{\Lambda^2}{m_\mathrm{t}^2}\right). \tag{A.16}$$

Since $m_\mathrm{t}/\Lambda < 1$, we perform a standard transformation of ${}_2F_1$ inverting the argument [42], so that we can use the ascending series expansion of ${}_2F_1$:

$$K_n = \frac{\Lambda^{n+1}}{n+1}\big(1+F(n)\big),$$
$$\int_0^\Lambda(\hat\Omega-1)\omega^n\,\mathrm{d}\omega = \frac{\Lambda^{n+1}}{n+1}F(n), \tag{A.17}$$

where

$$F(n) = {}_2F_1\left(-\frac{\sigma}{2},\frac{-1-n}{2};\frac{1-n}{2};-\frac{m_\mathrm{t}^2}{\Lambda^2}\right)-1$$
$$-(m_\mathrm{t}/\Lambda)^{n+1}\frac{\Gamma((n+1-\sigma)/2)\Gamma((1-n)/2)}{\Gamma(-\sigma/2)}. \tag{A.18}$$

We thus find Ξ_0 in (A.2) as

$$\Xi_0 = \Lambda\sum_{n=0}^{\infty}\frac{(-\mathrm{i}t\Lambda)^n}{(n+1)!}F(n). \tag{A.19}$$

To make this more explicit, we consider the real and imaginary parts of Ξ_0 separately. First,

$$\mathrm{Re}\,\Xi_0 = \Lambda\sum_{m=0}^{\infty}(-)^m\frac{(t\Lambda)^{2m}}{(2m+1)!}F(2m), \tag{A.20}$$

with $F(2m)$ in (A.18), where we substitute the ascending series of ${}_2F_1$:

$$\mathrm{Re}\,\Xi_0 = \kappa_\Lambda - m_\mathrm{t}\sum_{m=0}^{\infty}(-)^m(tm_\mathrm{t})^{2m}$$
$$\times\frac{\Gamma((2m+1-\sigma)/2)\Gamma(1/2-m)}{\Gamma(-\sigma/2)(2m+1)!}, \tag{A.21}$$
$$\kappa_\Lambda = \Lambda\sum_{n=0}^{\infty}\frac{(-)^n}{(2n)!}(\Lambda t)^{2n}$$
$$\times\sum_{k=1}^{\infty}\frac{(-)^k}{k!}\frac{\Gamma(k-\sigma/2)}{\Gamma(-\sigma/2)}\frac{(m_\mathrm{t}/\Lambda)^{2k}}{2n-2k+1}. \tag{A.22}$$

As for the imaginary part of Ξ_0, we find, analogously to (A.20),

$$\mathrm{Im}\,\Xi_0 = -\Lambda\sum_{m=0}^{\infty}(-)^m\frac{(t\Lambda)^{2m+1}}{(2m+2)!}F(2m+1+\varepsilon), \tag{A.23}$$

again with $F(2m+1+\varepsilon)$ in (A.18). Epsilon expansion is indicated here, as singularities occur in $F(n)$ at odd integer n, in a coefficient of the ascending series of ${}_2F_1$ as well as in $\Gamma((1-n)/2)$, which cancel if ε expanded [21, 32]. In (A.18), we put $n = 2m+1+\varepsilon$ and expand up to terms of $\mathrm{O}(\varepsilon)$:

$$\begin{aligned} &F(2m+1+\varepsilon) \\ &\quad= \frac{(-)^m}{m!}(m_\mathrm{t}/\Lambda)^{2m+2}\frac{\Gamma(m+1-\sigma/2)}{\Gamma(-\sigma/2)} \\ &\qquad\times\left[2\log\frac{m_\mathrm{t}}{\Lambda}+\psi(m+1-\sigma/2)-\psi(m+2)\right] \\ &\qquad+\frac{1+m}{\Gamma(-\sigma/2)} \\ &\qquad\times\sum_{\substack{k=1\\k\neq m+1}}^{\infty}\frac{\Gamma(k-\sigma/2)}{1+m-k}\frac{(-)^k}{k!}(m_\mathrm{t}/\Lambda)^{2k}, \end{aligned} \tag{A.24}$$

where ψ denotes the logarithmic derivative of the gamma function. On substituting this into (A.23), we obtain

$$\begin{aligned} \operatorname{Im}\Xi_0 &= -\chi_\Lambda + m_\mathrm{t}\sum_{k=1}^{\infty}(-)^k\binom{\sigma/2}{k}\frac{(m_\mathrm{t}t)^{2k-1}}{(2k-1)!} \\ &\quad\times\left(\frac{1}{2}\psi(k+1)-\frac{1}{2}\psi(k-\sigma/2)\right. \\ &\quad\left.-\log(m_\mathrm{t}/\Lambda)\right), \end{aligned} \tag{A.25}$$

$$\begin{aligned} \chi_\Lambda &= \Lambda\sum_{m=0}^{\infty}\frac{(-)^m}{(2m+1)!}(\Lambda t)^{2m+1} \\ &\quad\times\sum_{\substack{k=1\\k\neq m+1}}^{\infty}\binom{\sigma/2}{k}\frac{(m_\mathrm{t}/\Lambda)^{2k}}{2(m+1-k)}. \end{aligned} \tag{A.26}$$

Expansions (A.21) and (A.25) constitute the Taylor expansion of the low-frequency integral Ξ_0 in (A.2).

The small-t expansion of the high-frequency contribution Ξ_∞ in (A.2) is found by expanding $\hat{\Omega}(\omega)$ in ascending powers of m_t^2/ω^2, and applying term-by-term integration:

$$\Xi_\infty = m_\mathrm{t}\sum_{k=1}^{\infty}\binom{\sigma/2}{k}(m_\mathrm{t}/\Lambda)^{2k-1}\frac{\Gamma(-2k+1,\mathrm{i}\Lambda t)}{(\mathrm{i}\Lambda t)^{-2k+1}}. \tag{A.27}$$

Here, Γ is the incomplete gamma function as in (A.6); we substitute its ascending series

$$\begin{aligned} \frac{\Gamma(-2k+1,\mathrm{i}\Lambda t)}{(\mathrm{i}\Lambda t)^{-2k+1}} &= -\frac{(\mathrm{i}\Lambda t)^{2k-1}}{(2k-1)!}\big(\psi(2k)-\log(\mathrm{i}\Lambda t)\big) \\ &\quad-\sum_{\substack{n=0\\n\neq 2k-1}}^{\infty}\frac{(-)^n}{n!}\frac{(\mathrm{i}\Lambda t)^n}{n-2k+1}, \end{aligned} \tag{A.28}$$

valid for positive integer k. Principal values are assumed, $\log(\mathrm{i}\Lambda t) = \log(\Lambda|t|)+\operatorname{sign}(t)\mathrm{i}\pi/2$. In this way, we find

$$\begin{aligned} \operatorname{Re}\Xi_\infty &= -\kappa_\Lambda \\ &\quad+m_\mathrm{t}\frac{\pi}{2}\sum_{k=1}^{\infty}\binom{\sigma/2}{k}(-)^k\frac{(m_\mathrm{t}|t|)^{2k-1}}{(2k-1)!}, \end{aligned} \tag{A.29}$$

with series κ_Λ as in (A.22). κ_Λ drops out in $\operatorname{Re}\Xi = \operatorname{Re}\Xi_\infty + \operatorname{Re}\Xi_0$, cf. (A.21) and (A.29), so that the Taylor expansion of the real part of $\Xi(t)$ in (A.1) reads

$$\begin{aligned} \pi\Omega_\mathrm{reg}(t) &= \operatorname{Re}\Xi(t) \\ &= m_\mathrm{t}\frac{\pi}{2}\sum_{k=1}^{\infty}\binom{\sigma/2}{k}(-)^k\frac{(m_\mathrm{t}|t|)^{2k-1}}{(2k-1)!} \\ &\quad-m_\mathrm{t}\sum_{m=0}^{\infty}(-)^m(tm_\mathrm{t})^{2m} \\ &\quad\times\frac{\Gamma((2m+1-\sigma)/2)\Gamma(1/2-m)}{\Gamma(-\sigma/2)(2m+1)!}. \end{aligned} \tag{A.30}$$

The ascending t expansion of the imaginary part of the truncated integral Ξ_∞ in (A.2) is found like the real part (A.29), by substituting (A.28) into (A.27),

$$\begin{aligned} \operatorname{Im}\Xi_\infty &= \chi_\Lambda + m_\mathrm{t}\sum_{k=1}^{\infty}(-)^k\binom{\sigma/2}{k}\frac{(m_\mathrm{t}t)^{2k-1}}{(2k-1)!} \\ &\quad\times\big(\psi(2k)-\log(\Lambda|t|)\big), \end{aligned} \tag{A.31}$$

with series χ_Λ in (A.26). We thus obtain, by adding (A.25) and (A.31),

$$\begin{aligned} \operatorname{Im}\Xi(t) &= -\int_0^{\infty}(\hat{\Omega}-1)\sin(\omega t)\,\mathrm{d}\omega \\ &= m_\mathrm{t}\sum_{k=1}^{\infty}\frac{\Gamma(k-\sigma/2)}{\Gamma(-\sigma/2)}\frac{(m_\mathrm{t}t)^{2k-1}}{(2k)!(k-1)!} \\ &\quad\times\big(2\psi(2k)+\psi(k+1)-\psi(k-\sigma/2) \\ &\quad-2\log(m_\mathrm{t}|t|)\big). \end{aligned} \tag{A.32}$$

Expansions (A.30) and (A.32) constitute the ascending time series of integral $\Xi(t)$ in (A.1). The convergence radius of these series is infinite, but they are only efficient for $t \ll 1/m_\mathrm{t}$. The opposite limit is covered by the asymptotic expansion (A.13).

Appendix B: Tachyonic luminosity of electron plasmas at high temperature

B.1 Tachyonic power asymptotics

We average the radiant power $P^{\mathrm{T,L}}(\gamma)$ of individual inertial electrons in (7.3) over the electron density (6.3),

$$\big\langle P^{\mathrm{T,L}}\big\rangle_{\alpha,\beta} = A_{\alpha,\beta}\int_{\mu_\mathrm{t}}^{\infty}P^{\mathrm{T,L}}(\gamma)\,\mathrm{d}\hat{\rho}_{\alpha,\beta}(\gamma), \tag{B.1}$$

where μ_t is the electronic threshold Lorentz factor (6.2), and

$$\mathrm{d}\hat{\rho}_{\alpha,\beta}(\gamma) = \gamma^{-\alpha-1}\mathrm{e}^{-\beta\gamma}\sqrt{\gamma^2-1}\mathrm{d}\gamma. \tag{B.2}$$

To derive the high-temperature expansion ($\beta \ll 1$) of $\langle P^{\mathrm{T,L}}\rangle_{\alpha,\beta}$, we split integral (B.1) into a singular and regular part,

$$\langle P^{\mathrm{T,L}}\rangle_{\alpha,\beta} = A_{\alpha,\beta}\big(P^{\mathrm{T,L}}_{\mathrm{sing}} + P^{\mathrm{T,L}}_{\mathrm{reg}}\big), \tag{B.3}$$

$$\begin{aligned} P^{\mathrm{T,L}}_{\mathrm{sing}} &= \left(\int_1^\infty - \int_1^\Lambda\right) P^{\mathrm{T,L}}(\gamma)\,\mathrm{d}\hat{\rho}_{\alpha,\beta}(\gamma),\\ P^{\mathrm{T,L}}_{\mathrm{reg}} &= \int_{\mu_t}^\Lambda P^{\mathrm{T,L}}(\gamma)\,\mathrm{d}\hat{\rho}_{\alpha,\beta}(\gamma), \end{aligned} \tag{B.4}$$

with a cutoff parameter $\Lambda \gg \mu_t$. In $P^{\mathrm{T,L}}_{\mathrm{reg}}$, we substitute $P^{\mathrm{T,L}}(\gamma)$ as defined in (7.3) and (7.7), expand the exponential in (B.2), and use term-by-term integration to find the high-temperature expansion of this integral in ascending powers of β. In the following, only terms non-vanishing in the limit $\beta \to 0$ will be considered, so that we can put $\beta = 0$ in $P^{\mathrm{T,L}}_{\mathrm{reg}}$, which means to drop the exponential in density (B.2) when assembling $P^{\mathrm{T,L}}_{\mathrm{reg}}$:

$$P^{\mathrm{T,L}}_{\mathrm{reg},\beta=0} = \alpha_t\big(m_t^2c^4/\hbar\big)\big(f^{\mathrm{T,L}}_{\alpha,\Lambda} - g^{\mathrm{T,L}}_{\alpha,\Lambda} - h^{\mathrm{T,L}}_{\alpha,\Lambda}\big), \tag{B.5}$$

where we use the shortcuts, cf. (7.7),

$$\begin{aligned} f^{\mathrm{T,L}}_{\alpha,\Lambda} &= \int_{\mu_t}^\Lambda \left(\gamma^2 - \frac{1}{4}\frac{m_t^2}{m^2}\right)\gamma^{-\alpha-2}\frac{\hat{\omega}_{\max}^{2-2\sigma}(\gamma)}{2-2\sigma}\\ &\quad\times {}_2F_1\big(1-\sigma,1-\sigma;2-\sigma;-\hat{\omega}^2_{\max}(\gamma)\big)\,\mathrm{d}\gamma,\\ g^{\mathrm{T,L}}_{\alpha,\Lambda} &= \frac{m_t}{m}\int_{\mu_t}^\Lambda \gamma^{-\alpha-1}\frac{\hat{\omega}_{\max}^{3-2\sigma}(\gamma)}{3-2\sigma}\\ &\quad\times {}_2F_1\left(1-\sigma,\frac{3}{2}-\sigma;\frac{5}{2}-\sigma;-\hat{\omega}^2_{\max}(\gamma)\right)\mathrm{d}\gamma,\\ h^{\mathrm{T,L}}_{\alpha,\Lambda} &= \Delta^{\mathrm{T,L}}\int_{\mu_t}^\Lambda \gamma^{-\alpha-2}\frac{\hat{\omega}_{\max}^{2-2\sigma}(\gamma)}{2-2\sigma}\\ &\quad\times {}_2F_1\big(-\sigma,1-\sigma;2-\sigma;-\hat{\omega}^2_{\max}(\gamma)\big)\,\mathrm{d}\gamma. \end{aligned} \tag{B.6}$$

The singular part of the high-temperature series (comprising terms diverging for $\beta \to 0$) is obtained by substituting the asymptotic expansion (7.14) of $P^{\mathrm{T,L}}(\gamma \gg 1)$ into the two integrals defining $P^{\mathrm{T,L}}_{\mathrm{sing}}$ in (B.4). The subsequent term-by-term integration reduces to integrals of type

$$\begin{aligned} G_{\lambda,\beta} &= \int_1^\infty \gamma^{\lambda-1}\mathrm{e}^{-\beta\gamma}\,\mathrm{d}\gamma,\\ G^{(1)}_{\lambda,\beta} &= \int_1^\infty \gamma^{\lambda-1}\mathrm{e}^{-\beta\gamma}\log\gamma\,\mathrm{d}\gamma, \end{aligned} \tag{B.7}$$

$$\begin{aligned} H_{\lambda,\beta} &= \int_1^\Lambda \gamma^{\lambda-1}\mathrm{e}^{-\beta\gamma}\,\mathrm{d}\gamma,\\ H^{(1)}_{\lambda,\beta} &= \int_1^\Lambda \gamma^{\lambda-1}\mathrm{e}^{-\beta\gamma}\log\gamma\,\mathrm{d}\gamma, \end{aligned} \tag{B.8}$$

so that $P^{\mathrm{T,L}}_{\mathrm{sing}}$ can be assembled as, cf. (7.14),

$$\begin{aligned} P^{\mathrm{T,L}}_{\mathrm{sing}} &= \alpha_t\big(m_t^2c^4/\hbar\big)\big[G^{(1)}_{-\alpha+1,\beta} - H^{(1)}_{-\alpha+1,\beta}\\ &\quad + a_2(G_{-\alpha+1,\beta} - H_{-\alpha+1,\beta})\\ &\quad + a_1\big(G_{-\alpha,\beta} - H_{-\alpha,\beta}\big)\\ &\quad + a_{\mathrm{sing}}\big(G^{(1)}_{-\alpha-1,\beta} - H^{(1)}_{-\alpha-1,\beta}\big)\\ &\quad + a_0(G_{-\alpha-1,\beta} - H_{-\alpha-1,\beta})\\ &\quad + \mathrm{O}(G_{-\alpha-3,\beta}, H_{-\alpha-3,\beta})\big], \end{aligned} \tag{B.9}$$

where we insert the series expansions ($\beta \ll 1$) of integrals (B.7) and (B.8). The ascending β series of the integrals (B.7) read

$$\begin{aligned} G_{\lambda,\beta} &= \frac{\Gamma(\lambda,\beta)}{\beta^\lambda} = \frac{\Gamma(\lambda)}{\beta^\lambda} - \sum_{n=0}^\infty \frac{(-)^n\beta^n}{n!(n+\lambda)},\\ G^{(1)}_{\lambda,\beta} &= \frac{\mathrm{d}}{\mathrm{d}\lambda}G_{\lambda,\beta} = \frac{\Gamma(\lambda)}{\beta^\lambda}(\psi(\lambda)-\log\beta) + \sum_{n=0}^\infty \frac{(-)^n\beta^n}{n!(n+\lambda)^2}, \end{aligned} \tag{B.10}$$

where $\Gamma(\lambda,\beta)$ is the incomplete gamma function, and $\psi(\lambda)$ the logarithmic derivative $\Gamma'(\lambda)/\Gamma(\lambda)$ of the gamma function [42]. The series (B.10) are valid for real λ except at integer $\lambda \le 0$, where singularities emerge in the series coefficients requiring ε expansion; this will be studied in the next subsection. The Taylor series of the integrals $H_{\lambda,\beta}$ and $H^{(1)}_{\lambda,\beta}$ in (B.8) are obtained by expanding the exponential; we will only need the zeroth order ($\beta = 0$),

$$\begin{aligned} H_{\lambda,\beta} &= \frac{\Lambda^\lambda}{\lambda} - \frac{1}{\lambda} + \mathrm{O}(\beta),\\ H^{(1)}_{\lambda,\beta} &= \frac{\Lambda^\lambda}{\lambda}\left(\log\Lambda - \frac{1}{\lambda}\right) + \frac{1}{\lambda^2} + \mathrm{O}(\beta). \end{aligned} \tag{B.11}$$

By substituting expansions (B.10) and (B.11) into (B.9), we find the singular part of the power (B.3):

$$P^{\mathrm{T,L}}_{\mathrm{sing}} = \alpha_t\big(m_t^2c^4/\hbar\big)\big(P^{\mathrm{T,L}}_{\alpha,\beta} - P^{\mathrm{T,L}}_{\alpha,\Lambda}\big), \tag{B.12}$$

with the shortcuts

$$\begin{aligned} P^{\mathrm{T,L}}_{\alpha,\beta} &= \frac{\Gamma(-\alpha+1)}{\beta^{-\alpha+1}}\left(\log\frac{1}{\beta} + \psi(-\alpha+1) + a_2\right)\\ &\quad + a_1\frac{\Gamma(-\alpha)}{\beta^{-\alpha}} + \frac{\Gamma(-\alpha-1)}{\beta^{-\alpha-1}} \end{aligned}$$

$$\times\left(a_{\text{sing}}\log\frac{1}{\beta}+a_{\text{sing}}\psi(-\alpha-1)+a_0\right)+\mathrm{O}\left(\frac{1}{\beta^{-\alpha-3}},\beta\right), \tag{B.13}$$

and

$$P^{\text{T,L}}_{\alpha,\Lambda}=\frac{\Lambda^{1-\alpha}}{1-\alpha}\left(\log\Lambda-\frac{1}{1-\alpha}+a_2\right)-a_1\frac{\Lambda^{-\alpha}}{\alpha}-\frac{\Lambda^{-\alpha-1}}{\alpha+1}\left(a_{\text{sing}}\log\Lambda+\frac{a_{\text{sing}}}{\alpha+1}+a_0\right)+\mathrm{O}\left(\Lambda^{-\alpha-3}\right). \tag{B.14}$$

$P^{\text{T,L}}_{\alpha,\beta}$ is the contribution of the G terms in (B.9), and $P^{\text{T,L}}_{\alpha,\Lambda}$ of the H terms, up to a constant which cancels in the difference (B.12). This expansion is valid for noninteger α. The constant term in the high-temperature expansion of $P^{\text{T,L}}_{\text{sing}}+P^{\text{T,L}}_{\text{reg}}$ in (B.3) is calculated as $P^{\text{T,L}}_{\text{reg},\beta=0}-\alpha_{\text{t}}(m_{\text{t}}^2c^4/\hbar)P^{\text{T,L}}_{\alpha,\Lambda}$, with large Λ, cf. (B.5). If the error term $\mathrm{O}(\Lambda^{-\alpha-3})$ in (B.14) does not vanish for $\Lambda\to\infty$, which happens for electron indices $\alpha<-3$, we would have to calculate higher orders in the expansions (7.14) and (B.9) to extract the constant term. At these electron indices, however, the leading orders in (B.13) largely overpower the constant term in the expansion. If $\alpha>1$, then $P^{\text{T,L}}_{\alpha,\beta}$ in (B.13) vanishes for $\beta\to0$, and so does $P^{\text{T,L}}_{\alpha,\Lambda}$ in (B.14) for $\Lambda\to\infty$. In (B.6), we may thus extend the integration boundary to $\Lambda=\infty$, and $P^{\text{T,L}}_{\text{reg},\beta=0}$ in (B.5) is the leading (constant) term of the high-temperature expansion, provided that $\alpha>1$. Typically, the electron index ranges in the interval $-2\le\alpha\le2$.

B.2 High-temperature expansion of the tachyonic power at integer electron index

For integer electron index α, the expansion (B.12)–(B.14) of $P^{\text{T,L}}_{\text{sing}}$ needs to be modified, as singularities arise in the series coefficients, which can be extracted by way of ε expansion. In series (B.10), we substitute $\lambda=-k+\varepsilon$, with integer $k\ge0$, to find

$$\begin{aligned}G_{-k+\varepsilon,\beta}&=\frac{\Gamma(-k+\varepsilon)}{\beta^{-k+\varepsilon}}-\frac{1}{\varepsilon}\frac{(-)^k}{k!}\beta^k-\sum_{\substack{n=0\\n\neq k}}^{\infty}\frac{(-)^n\beta^n}{n!(n-k)}+\mathrm{O}(\varepsilon),\\ G^{(1)}_{-k+\varepsilon,\beta}&=\frac{\mathrm{d}}{\mathrm{d}\varepsilon}\frac{\Gamma(-k+\varepsilon)}{\beta^{-k+\varepsilon}}+\frac{1}{\varepsilon^2}\frac{(-)^k}{k!}\beta^k+\sum_{\substack{n=0\\n\neq k}}^{\infty}\frac{(-)^n\beta^n}{n!(n-k)^2}+\mathrm{O}(\varepsilon).\end{aligned} \tag{B.15}$$

The $\mathrm{O}(\varepsilon^2)$ expansion of the gamma function,

$$\Gamma(-k+\varepsilon)=\frac{(-)^k}{k!}\left[\frac{1}{\varepsilon}+\psi(k+1)+\frac{\varepsilon}{2}\left(\psi^2(k+1)-\psi'(k+1)+\frac{\pi^2}{3}\right)+\mathrm{O}\left(\varepsilon^2\right)\right], \tag{B.16}$$

valid for integer $k\ge0$, can be used to calculate the ε derivative $\Gamma'(-k+\varepsilon)$ up to terms of $\mathrm{O}(\varepsilon)$. We also note the psi function and its derivative at positive integers [42],

$$\begin{aligned}\psi(k+1)&=-\gamma_{\text{E}}+1+\frac{1}{2}+\cdots+\frac{1}{k},\\ \psi'(k+1)&=\frac{\pi^2}{6}-\left(1+\frac{1}{2^2}+\cdots+\frac{1}{k^2}\right),\end{aligned} \tag{B.17}$$

in particular $\psi(1)=-\gamma_{\text{E}}$, where $\gamma_{\text{E}}\approx0.5772$ is Euler's constant, and $\psi'(1)=\pi^2/6$. We thus find, for $k\ge0$, the ε expansions

$$\begin{aligned}\frac{\Gamma(-k+\varepsilon)}{\beta^{-k+\varepsilon}}&=\frac{(-)^k}{k!}\beta^k\left(\frac{1}{\varepsilon}-\log\beta+\psi(k+1)+\mathrm{O}(\varepsilon)\right),\\ \frac{\mathrm{d}}{\mathrm{d}\varepsilon}\frac{\Gamma(-k+\varepsilon)}{\beta^{-k+\varepsilon}}&=\frac{(-)^k}{k!}\beta^k\left(-\frac{1}{\varepsilon^2}+\frac{1}{2}\log^2\beta-\psi(k+1)\log\beta+\frac{1}{2}\psi^2(k+1)-\frac{1}{2}\psi'(k+1)+\frac{\pi^2}{6}+\mathrm{O}(\varepsilon)\right).\end{aligned} \tag{B.18}$$

On substituting this into (B.15), the ε poles cancel, and we can perform the limit $\varepsilon\to0$ to obtain the ascending β series of the integrals (B.7) at $\lambda=-k$,

$$\begin{aligned}G_{-k,\beta}&=\frac{(-)^k}{k!}\beta^k\big(-\log\beta+\psi(k+1)\big)-\sum_{\substack{n=0\\n\neq k}}^{\infty}\frac{(-)^n\beta^n}{n!(n-k)},\\ G^{(1)}_{-k,\beta}&=\frac{(-)^k}{k!}\beta^k\left[\frac{1}{2}\log^2\beta-\psi(k+1)\log\beta+\frac{1}{2}\psi^2(k+1)-\frac{1}{2}\psi'(k+1)+\frac{\pi^2}{6}\right]+\sum_{\substack{n=0\\n\neq k}}^{\infty}\frac{(-)^n\beta^n}{n!(n-k)^2},\end{aligned} \tag{B.19}$$

valid for integer $k\ge0$. For negative integer k (or positive integer λ), we can still use series (B.10). Finally, at $\lambda=0$, we replace (B.11) by

$$\begin{aligned}H_{0,\beta}&=\log\Lambda+\mathrm{O}(\beta),\\ H^{(1)}_{0,\beta}&=\frac{1}{2}\log^2\Lambda+\mathrm{O}(\beta).\end{aligned} \tag{B.20}$$

The leading orders of $P^{\mathrm{T,L}}_{\mathrm{sing}}$ in (B.3) can thus be calculated by substituting the respective series (B.10) and (B.11) or (B.19) and (B.20) into (B.9). $P^{\mathrm{T,L}}_{\mathrm{reg},\beta=0}$ in (B.5) and (B.6) also applies for integer α. In the following, we list the leading orders of the high-temperature expansion of $P^{\mathrm{T,L}}_{\mathrm{sing}}$ in (B.3) for integer electron indices $-2 \le \alpha \le 2$.

For $\alpha = -2$(thermal equilibrium) and $\alpha = -1$, we find $P^{\mathrm{T,L}}_{\mathrm{sing}} = \alpha_{\mathrm{t}}(m_{\mathrm{t}}^2c^4/\hbar)P^{\mathrm{T,L}}_{\alpha,\beta}$, where

$$P^{\mathrm{T,L}}_{\alpha=-2,\beta} = \frac{2}{\beta^3}\left(\log\frac{1}{\beta} + \frac{3}{2} - \gamma_{\mathrm{E}} + a_2\right) + \frac{a_1}{\beta^2} + \mathrm{O}\left(\frac{\log\beta}{\beta}\right), \tag{B.21}$$

$$P^{\mathrm{T,L}}_{\alpha=-1,\beta} = \frac{1}{\beta^2}\left(\log\frac{1}{\beta} + 1 - \gamma_{\mathrm{E}} + a_2\right) + \frac{a_1}{\beta} + \mathrm{O}\left(\log^2\beta\right). \tag{B.22}$$

The H terms in (B.9) need not be considered, as they only affect the constant term in the expansions, which is smaller than the indicated error terms. $P^{\mathrm{T,L}}_{\mathrm{reg},\beta=0}$ in (B.5) can be ignored for the same reason, so that the averaged power is found as $\langle P^{\mathrm{T,L}}\rangle_{\alpha,\beta} \sim A_{\alpha,\beta}\alpha_{\mathrm{t}}(m_{\mathrm{t}}^2c^4/\hbar)P^{\mathrm{T,L}}_{\alpha,\beta}$, cf. (B.3).

For $\alpha = 0$, we obtain the singular power as $P^{\mathrm{T,L}}_{\mathrm{sing}} = \alpha_{\mathrm{t}}(m_{\mathrm{t}}^2c^4/\hbar)(P^{\mathrm{T,L}}_{\alpha,\beta} - P^{\mathrm{T,L}}_{\alpha,\Lambda})$, cf. (B.12), where

$$\begin{aligned} P^{\mathrm{T,L}}_{\alpha=0,\beta} &= \frac{1}{\beta}\left(\log\frac{1}{\beta} - \gamma_{\mathrm{E}} + a_2\right) + a_1\left(\log\frac{1}{\beta} - \gamma_{\mathrm{E}}\right) + \mathrm{O}\left(\beta\log^2\beta\right), \\ P^{\mathrm{T,L}}_{\alpha=0,\Lambda} &= \Lambda(\log\Lambda - 1 + a_2) + a_1\log\Lambda - \frac{1}{\Lambda}(a_{\mathrm{sing}}\log\Lambda + a_{\mathrm{sing}} + a_0) + \mathrm{O}\left(\Lambda^{-3}\right). \end{aligned} \tag{B.23}$$

In this case, $P^{\mathrm{T,L}}_{\mathrm{reg},\beta=0}$ in (B.5) has to be included in $\langle P^{\mathrm{T,L}}\rangle_{\alpha,\beta} \sim A_{\alpha,\beta}(P^{\mathrm{T,L}}_{\mathrm{sing}} + P^{\mathrm{T,L}}_{\mathrm{reg},\beta=0})$, since the constant term $P^{\mathrm{T,L}}_{\mathrm{reg},\beta=0} - \alpha_{\mathrm{t}}(m_{\mathrm{t}}^2c^4/\hbar)P^{\mathrm{T,L}}_{\alpha,\Lambda}$ (which is finite for $\Lambda\to\infty$) dominates the error term $\mathrm{O}(\beta\log^2\beta)$. The same holds for $\alpha = 1$, with (B.23) replaced by

$$\begin{aligned} P^{\mathrm{T,L}}_{\alpha=1,\beta} &= \frac{1}{2}\log^2\frac{1}{\beta} + (a_2 - \gamma_{\mathrm{E}})\log\frac{1}{\beta} + \frac{1}{2}\gamma_{\mathrm{E}}^2 + \frac{\pi^2}{12} - \gamma_{\mathrm{E}}a_2 + \mathrm{O}(\beta\log\beta), \\ P^{\mathrm{T,L}}_{\alpha=1,\Lambda} &= \frac{1}{2}\log^2\Lambda + a_2\log\Lambda - \frac{a_1}{\Lambda} - \frac{1}{\Lambda^2}\left(\frac{a_{\mathrm{sing}}}{2}\log\Lambda + \frac{a_{\mathrm{sing}}}{4} + \frac{a_0}{2}\right) + \mathrm{O}\left(\Lambda^{-4}\right). \end{aligned} \tag{B.24}$$

At $\alpha = 2$, we find $P^{\mathrm{T,L}}_{\alpha=2,\beta} = \mathrm{O}(\beta\log^2\beta)$ and

$$P^{\mathrm{T,L}}_{\alpha=2,\Lambda} = -\frac{1}{\Lambda}(\log\Lambda + 1 + a_2) - \frac{a_1}{2}\frac{1}{\Lambda^2} - \frac{1}{\Lambda^3}\left(\frac{a_{\mathrm{sing}}}{3}\log\Lambda + \frac{a_{\mathrm{sing}}}{9} + \frac{a_0}{3}\right) + \mathrm{O}\left(\Lambda^{-5}\right). \tag{B.25}$$

$P^{\mathrm{T,L}}_{\mathrm{reg},\beta=0}$ in (B.5) is finite for $\Lambda\to\infty$, and $P^{\mathrm{T,L}}_{\alpha=2,\Lambda}$ vanishes, so that $\langle P^{\mathrm{T,L}}\rangle_{\alpha,\beta} \sim A_{\alpha,\beta}P^{\mathrm{T,L}}_{\mathrm{reg},\beta=0}$, which applies in fact for all real $\alpha > 1$, cf. (B.13). Even though the integrals (B.6) converge, it is efficient to employ $P^{\mathrm{T,L}}_{\alpha=2,\Lambda}$ in the numerical integration.

We still have to settle the normalization factor $A_{\alpha,\beta}$ of the electron density (6.3), which enters in the power average (B.1). We note $A_{\alpha,\beta} = n_{\mathrm{e}}/K_{\alpha,\beta}$, where n_{e} is the electron number and $K_{\alpha,\beta} = \int_1^\infty \mathrm{d}\hat{\rho}_{\alpha,\beta}(\gamma)$, cf. (B.2). The high-temperature expansion of $K_{\alpha,\beta}$ reads [32]

$$K_{\alpha,\beta} = \beta^{\alpha-1}\sum_{k=0}^{\infty}(-)^k\frac{(1/2)_k}{k!}\Gamma(1-\alpha-2k)\beta^{2k} + c_{0,\alpha} + \mathrm{O}(\beta), \tag{B.26}$$

where $(1/2)_k$ denotes the falling factorial, $(a)_k = a(a-1)\cdots(a-k+1)$, $(a)_0 = 1$, and

$$c_{0,\alpha} = \frac{\sqrt{\pi}}{2}\frac{\Gamma((\alpha-1)/2)}{\alpha\Gamma(\alpha/2)}. \tag{B.27}$$

Hence, $K_{\alpha,\beta} \sim \Gamma(1-\alpha)/\beta^{1-\alpha}$ for $\alpha < 1$, and a constant high-temperature limit $K_{\alpha,\beta} \sim c_{0,\alpha}$ is attained for $\alpha > 1$. At integer electron index α, singularities arise in the series coefficients in (B.26), which have to be ε expanded to obtain, for instance [32],

$$\begin{aligned} K_{\alpha=1,\beta} &= \log\frac{2}{\beta} - \gamma_{\mathrm{E}} - 1 + \mathrm{O}(\beta), \\ K_{\alpha=2,\beta} &= \frac{\pi}{4} + \mathrm{O}(\beta\log\beta). \end{aligned} \tag{B.28}$$

In the high-temperature regime, the temperature dependence of the power average $\langle P^{\mathrm{T,L}}\rangle_{\alpha,\beta}$ in (B.3) is weak, since the leading orders of $P^{\mathrm{T,L}}_{\mathrm{sing}} + P^{\mathrm{T,L}}_{\mathrm{reg}}$ and $K_{\alpha,\beta}$ differ by at most a logarithmic term, cf. (7.17).

References

1. G. Wentzel, *Quantum Theory of Fields* (Interscience, New York, 1949)
2. R. Tomaschitz, Class. Quantum Gravity **18**, 4395 (2001)
3. R. Tomaschitz, Europhys. Lett. **89**, 39002 (2010)
4. S. Tanaka, Prog. Theor. Phys. **24**, 171 (1960)
5. K. Kamoi, S. Kamefuchi, Prog. Theor. Phys. **45**, 1646 (1971)
6. H.M. Fried, Y. Gabellini, arXiv:0709.0414
7. R. Tomaschitz, Eur. Phys. J. B **17**, 523 (2000)
8. R. Tomaschitz, Astropart. Phys. **27**, 92 (2007)

9. R. Tomaschitz, Appl. Phys. B (2010). doi:10.1007/s00340-010-4182-8
10. B.M. Bolotovskiĭ, V.P. Bykov, Sov. Phys. Usp. **33**, 477 (1990)
11. B.M. Bolotovskiĭ, A.V. Serov, Radiat. Phys. Chem. **75**, 813 (2006)
12. A.V. Bessarab et al., IEEE Trans. Plasma Sci. **32**, 1400 (2004)
13. A.V. Bessarab et al., Radiat. Phys. Chem. **75**, 825 (2006)
14. M.S. Bigelow, N.N. Lepeshkin, R.W. Boyd, Science **301**, 200 (2003)
15. T. Baba, Nature Photonics **2**, 465 (2008)
16. L. Thévenaz, Nature Photonics **2**, 474 (2008)
17. G. Dolling et al., Science **312**, 892 (2006)
18. G.M. Gehring et al., Science **312**, 895 (2006)
19. Y. Kaneko et al., Astrophys. J. **677**, 1168 (2008)
20. R. Tomaschitz, Eur. Phys. J. C **49**, 815 (2007)
21. R. Tomaschitz, Ann. Phys. **322**, 677 (2007)
22. R. Tomaschitz, Physica B **404**, 1383 (2009)
23. L.D. Landau, E.M. Lifshitz, *Electrodynamics of Continuous Media* (Pergamon, Oxford, 1984)
24. E.J. Post, *Formal Structure of Electromagnetics* (Dover, New York, 1997)
25. M. Born, E. Wolf, *Principles of Optics* (Cambridge University Press, Cambridge, 2003)
26. R. Tomaschitz, Opt. Commun. **282**, 1710 (2009)
27. R. Tomaschitz, Europhys. Lett. **84**, 19001 (2008)
28. R. Tomaschitz, Physica A **307**, 375 (2002)
29. R. Tomaschitz, Eur. Phys. J. D **32**, 241 (2005)
30. S. Ichimaru, Rev. Mod. Phys. **65**, 255 (1993)
31. U. Teubner, P. Gibbon, Rev. Mod. Phys. **81**, 445 (2009)
32. R. Tomaschitz, Physica A **385**, 558 (2007)
33. R. Tomaschitz, Physica A **387**, 3480 (2008)
34. R. Tomaschitz, Physica B **405**, 1022 (2010)
35. J.L. Racusin et al., Nature **455**, 183 (2008)
36. A.A. Abdo et al., Science **323**, 1688 (2009)
37. N.R. Tanvir et al., Nature **461**, 1254 (2009)
38. A. Minguzzi, M.P. Tosi, Physica B **300**, 27 (2001)
39. R. Tomaschitz, Phys. Lett. A **372**, 4344 (2008)
40. R. Tomaschitz, Europhys. Lett. **85**, 29001 (2009)
41. R. Tomaschitz, Eur. Phys. J. C **45**, 493 (2006)
42. W. Magnus, F. Oberhettinger, R.P. Soni, *Formulas and Theorems for the Special Functions of Mathematical Physics* (Springer, New York, 1966)
43. R. Tomaschitz, Phys. Lett. A **366**, 289 (2007)